

Visualize Dynamic Sensitivity of Biological Systems

Shing-Jen Wu^{1,*} and Sing-Yu Lu²

^{1,2}Department of Electrical Engineering Da-Yeh University, 168 University Rd., Dacun
Changhua 51591, Taiwan, R.O.C

Abstract

Dynamic Sensitivity analysis is important for us to realize the instantaneous response of systems to perturbation on system parameters or independent variables (modellable environmental conditions). Sensitivity analysis in L_2 or L_1 norm additionally gives people a guideline to choose critical parameters for the transient behavior of underlying systems. In this study, the Simulink (a visualization toolbox in Matlab software) is used to visualize both nonlinear differential equations of sensitivity and system in block diagrams and then to achieve model-based sensitivity analysis. The dynamic sensitivity of each dependent variable is denoted as a *single subsystem block*. In this way a large-scale system with n dependent variables (called state variables or states) is expressed as n *subsystem blocks*. A reversible Michaelis-Menten kinetics module is to describe the proposed Simulink-based resolution clearly. The instantons effect of parametric perturbation on system behaviors observed and the ensemble parametric influence ranking on *system transient behavior* is obtained. Additionally, the *static* sensitivity for various independent variable sets is sufficiently discussed to realize the tendency of steady states to parametric perturbations and get the limiting influence strength.

Keywords: system analysis, computational analysis, computational biology, graphical models, biochemistry, systems biology

Date of Submission: 09-10-2022

Date of Acceptance: 22-10-2022

I. INTRODUCTION

Modelling, analysis and control are a trilogy for solving practical problems from a viewpoint of quantity. Voit took a deep review of 752 papers in various nonlinear models, model designs, parameter estimations and diagnostics of biological system theory [1]. Sriyudthsak and coworkers reviewed various biological system models and their limitations [2]. Modelling is extensively used in biochemical studies nowadays. Bartocci and Lio reviewed various computational modeling and analysis technologies and brought forward that ordinary differential equations will get more attention [3]. We proposed that fuzzy models have the potential to be a suitable model candidate because biological systems are always subject to uncertainty and noise [4]. S-systems (power-law-based structure) and Michaelis-Menten systems are two popular differential equation-based biological models. Michaelis-Menten systems describe individual fluxes as nonlinear hill kinetics (for example, the reversible Michaelis-Menten kinetics v_{ij}^+ , $v_{ij}^- = \frac{V_{ij}^{max}}{1+x_i/K_{ij}+x_j/K_{-ij}}$ where x_i, x_j are dependent variables, and $V_{ij}^{max}, K_{ij}, K_{-ij}$ are, respectively, the maximum reaction rate at saturating substrate

concentration, the Michaelis constants of the forward and backward reactions.) Liu and coworkers used the S-system to describe p53 signaling pathway mechanism [5]. Tyson and coworkers successfully developed Michaelis-Menten kinetics to capture the dynamic movement of a mammalian cell from autophagy to apoptosis [6] and the interactions of sense and antisense transcription on mammalian circadian rhythms [7], and to describe eukaryotic cell cycles [8] and cell volume growth and size control via inhibitor dilution and titration of nuclear sites [9]. We integrated Michaelis-Menten modules and petri-net modules to predict the dynamic behavior of the antigrowth signal-induced cell cycle and multi-stream growth and apoptotic signal transduction mechanisms [10].

Sensitivity analysis is a systematic investigation of system response to perturbation on system inputs or system parameters. Time-varying parametric sensitivity analysis (dynamic parametric sensitivity) gives us quantitatively information for structural uncertainty (parameter perturbation), which improves our understanding in dynamic behavior of underlying systems, and is useful to identify bottleneck enzymes (critical parameter-related enzymes or reaction steps). Chen et al.

observed that parameter sensitivity ranking in bifurcation point location variation (deterministic models) is closely correlated to energy barrier of a cell from alive to death (stochastic models) [11]. There are two kinds of approaches for sensitivity analysis (global sensitivity and local sensitivity). Zi reviewed various approaches of both sensitivity analysis [12]. Borgonovo and Pllischke emphasized that sensitivity analysis is a crucial step of modelling and result analysis in communication processes [13]. They took an overview for various available methods in both sensitivities, and discussed Tornado diagrams for local sensitivity, screening methods, variance-based, moment-independent and information-based methods for global sensitivity. Global sensitivity analysis discusses system response to *simultaneous* parameter variations or input variation *in a large range*. Sumner et al. introduced functional principal component analysis into current global sensitivity methods to identify a number of interesting features of insulin signalling pathways [14]. Wong et al. used global sensitivity analysis for debris flow energy dissipation process to reduce hazards [15]. Local sensitivity analysis is for system response to *infinitesimal* perturbation of *single* parameter or input. Hu and Yuan used local dynamic sensitivity to analyze coupled MAPK and P13K signal transduction pathways and demonstrated that local dynamic analysis is a good way for analyzing complex biological systems [16]. Local sensitivity analysis needs to solve sensitivity differential equations and system differential equations. Therefore, it is impossible to find out an exact

solution. Wu et al. used modification collocation methods, wherein Lagrange polynomials were used as shape functions, to transform differential equations to algebraic equations and developed a corresponding algorithm to solve this issue [17]. Shiraishi et al. developed a software for calculation of dynamic sensitivity (SoftCADs) to simultaneously solve nonlinear ordinary differential equations wherein variable-order and variable-step Taylor series were used [18]. Shiraishi et al. further improved SoftCADs in accuracy and speed [19]. Perumal and Gunawan proposed dynamical pathway-based sensitivity analysis which perturbed pathway kinetics and considered persistent perturbation and impulse perturbations at different time points to find out dominant pathways and transient shifts in rating-controlled mechanisms [20]. Sriyudthsak and Shiraishi used *dynamic logarithmic gain (normalized sensitivity)* to identify bottleneck enzymes in ethanol fermentation systems [21] and believed that normalized sensitivity was the best bottleneck ranking indicator [22]. Sriyudthsaket al. further analyzed dynamic logarithmic gain of a biosynthetic pathway with three aromatic amino acids and concluded that dynamic logarithmic gain could give additional insights on transient behavior [23]. In this study, we visualize both system and sensitivity differential equations in block diagrams to get the local dynamic parametric sensitivity. Ensemble influence of parameter perturbation to system transient behavior is further discussed. We also discuss the response in steady state. For clarity, a *small* reversible Michaelis-Menten kinetics module is used as our case.

II. METHODS

Perturbation theorem [24]

For a system described as $\dot{X}(t) = f(X(t), t, \theta^0)$ with $X(t_0) = X_0$, where the state variable $X(t) = [x_1, \dots, x_n]^T$, t denotes the time and $\theta^0 \in R^m$ is the nominal values of real parameter vectors $\theta = [\theta_1, \dots, \theta_m]^T$. The nominal solution denoted as φ^0 is a time function parametrized by t_0, X_0 and θ^0 . We now slightly perturb parameters from θ^0 to $\theta^0 + \delta\theta$. The solution for the perturbed system $\dot{X}(t) = f(X(t), t, \theta^0 + \delta\theta)$ becomes $\varphi^0 + \delta\varphi$. We then obtain the following Taylor expansion [24],

$$\begin{aligned} \dot{\varphi}^0(t) + \delta\dot{\varphi}(t) &= f(\varphi^0 + \delta\varphi, t, \theta^0 + \delta\theta) \\ &= f(\varphi^0, t, \theta^0) + D_1 f|_{(\varphi^0, t, \theta^0)} \cdot \delta\varphi + D_3 f|_{(\varphi^0, t, \theta^0)} \cdot \delta\theta + H.O.T., \end{aligned} \quad (1)$$

where $D_i f|_{(\varphi^0, t, \theta^0)}$, $i = 1, 3$ denotes the derivative of f with respect to the i th argument ($i = 1$ for state variables φ and $i = 3$ for parameters θ) and “H.O.T” denotes the higher-order terms in $\delta\varphi$ and $\delta\theta$. The equation is approximately as

$$\delta\dot{\varphi}(t) = D_1 f|_{(\varphi^0, t, \theta^0)} \cdot \delta\varphi + D_3 f|_{(\varphi^0, t, \theta^0)} \cdot \delta\theta. \quad (2)$$

We further use a vector $S = \frac{\delta\varphi}{\delta\theta}$ to denote parametric dynamic sensitivity and obtain

$$\frac{dS}{dt}(t) = JS(t) + B, \quad (3)$$

where $J = D_1 f|_{(\varphi^0, t, \theta^0)}$ is the Jacobian matrix and $B = D_3 f|_{(\varphi^0, t, \theta^0)}$.

If a system possesses n dependent variables with m parameters, then there are nm elements in the sensitivity matrix S . However, most of elements in the matrix S are zero. For example, a branchpoints metabolic pathway in Eq. (1) [25]: (there are four dependent variables and eight parameters.)

$$\begin{aligned} \dot{x}_1 &= k_3 x_2 x_4 - k_4 x_1 - \frac{V_5 x_1}{K_{m5} + x_1}, \\ \dot{x}_2 &= k_2 x_6 + k_1 x_5 + k_4 x_1 - k_3 x_2 x_4, \\ \dot{x}_3 &= \frac{V_5 x_1}{K_{m5} + x_1} - \frac{V_6 x_3}{K_{m6} + x_3}, \\ \dot{x}_4 &= \frac{V_6 x_3}{K_{m6} + x_3} + k_4 x_1 - k_3 x_2 x_4. \end{aligned} \quad (4)$$

The sensitivity matrix S has 32 elements, but 16 elements are zero. We observe that for the state variable x_1 only the sensitivity of x_1 to the parameters k_3, k_4, V_5, K_{m5} is not zero. The same is that for the state variable x_2 only the sensitivity of x_2 to the parameters k_1, k_2, k_3, k_4 is not zero, for the state variable x_3 only the sensitivity of x_3 to the parameters V_5, K_{m5}, V_6, K_{m6} is nonzero and for the state variable x_4 only the sensitivity of x_3 to the parameters k_3, k_4, V_6, K_{m6} is nonzero.

Block diagram-based visualization [26]

Simulink is a toolbox of Matlab (MATrix LABORatory, a software developed by The MathWorks Company). The toolbox provides an environment to build up block diagrams of underlying systems for model-based testing, analysis and design. Block diagrams are a kind of systems models in which the principal parts or functions are shown as blocks connected to each other by directed lines, showing the flow of signals. Researchers are able to draw block diagrams in the Simulink environment to achieve modelling, simulating and analyzing multi-domain dynamic systems.

III. RESULTS AND DISCUSSION

Voit and coworkers noted that “Most large systems in biology are modular and exhibit possibly generic design features at different levels... so that a true understanding of ever smaller functional modules greatly enhances the understanding of the system as a whole” [1]. In this study, a reversible MM kinetics module is used to describe the proposed method clearly.

■ Visualize Parametric Dynamic Sensitivity

Amphibolic pathways possess metabolism in both degradative and biosynthesis phases; for example, Embeden-Meyerhof pathways, Krebs cycles, pentose phosphate pathways, Entner-Doudoroff pathways and citric acid cycles. We here consider an *in silico* reversible pathway in Fig. 1. The dynamic behavior of the amphibolic pathway is described as reversible Michaelis-Menten kinetics in Eq. (5) [27, 28]. The x_4 and x_3 are independent variables which remain constant during the entire experiment. The x_1 and x_2 are dependent variables. The concentration change of x_1 is the net influx r_{41} minus the net efflux r_{12} and the change in x_2 is the net flux r_{12} minus the net efflux r_{23} .

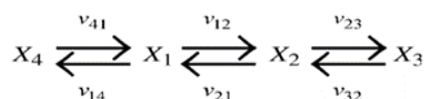


Figure 1: A reversible pathway [23, 24].

$$\begin{aligned} \dot{x}_1 &= (v_{41} - v_{14}) - (v_{12} - v_{21}) = r_{41} - r_{12}, \\ \dot{x}_2 &= (v_{12} - v_{21}) - (v_{23} - v_{32}) = r_{12} - r_{23}, \end{aligned} \quad (5)$$

where $v_{41} = \frac{V_{41}^{max} x_4}{1 + x_4/K_{41} + x_1/K_{41}}$, $v_{14} = \frac{V_{14}^{max} x_1}{1 + x_4/K_{14} + x_1/K_{14}}$, $v_{12} = \frac{V_{12}^{max} x_1}{1 + x_1/K_{12} + x_2/K_{12}}$, $v_{21} = \frac{V_{21}^{max} x_2}{1 + x_1/K_{21} + x_2/K_{21}}$, $v_{23} = \frac{V_{23}^{max} x_2}{1 + x_2/K_{23} + x_3/K_{23}}$, $v_{32} = \frac{V_{32}^{max} x_3}{1 + x_2/K_{32} + x_3/K_{32}}$. The nominal values of rate parameters are $V_{12}^{max} = V_{21}^{max} = 50$, $V_{14}^{max} = V_{41}^{max} = 60$, $V_{23}^{max} = V_{32}^{max} = 140$; the nominal values of Michaelis parameters are $K_{12} = K_{21} = 1$, $K_{14} = K_{41} = 1$, $K_{32} = K_{23} = 0.5$ for forward reactions and $K_{-12} = K_{-21} = 6$, $K_{-14} = K_{-41} = 8$, $K_{-32} = K_{-23} = 5$ for reverse reactions. The equation and the values of the associated parameters are cited from Sorribas and Savageau’s paper [27] and Liu and Wang’s paper [28]. (See the supplemental file of our previously paper [29].)

This system possesses two dependent variables (state variables or states) and eighteen parameters. So, the parametric sensitivity matrix S has thirty-six elements, but twelve elements are zero. Additionally, the value of associate parameters for forward and reverse equations are always the same. (See the supplemental file of our previously paper [29] in a comparison of the papers [27], [28] and [29] in symbols, equations and the values of the associated parameters.) So, we rewrite Eq. (5) as

$$\begin{aligned} \dot{x}_1 &= r_{41} - r_{12} = \frac{V_{41}^{max}(x_4 - x_1)}{1 + x_4/K_{41} + x_1/K_{-41}} - \frac{V_{12}^{max}(x_1 - x_2)}{1 + x_1/K_{12} + x_2/K_{-12}}, \\ \dot{x}_2 &= r_{12} - r_{23} = \frac{V_{12}^{max}(x_1 - x_2)}{1 + x_1/K_{12} + x_2/K_{-12}} - \frac{V_{23}^{max}(x_2 - x_3)}{1 + x_2/K_{23} + x_3/K_{-23}}. \end{aligned} \quad (6)$$

The twenty-four nonzero elements in sensitivity matrix S is further reduced to twelve elements. For the state variable x_1 only the sensitivity of x_1 to the parameters $K_{41}, K_{-41}, V_{41}^{max}, K_{12}, K_{-12}, V_{12}^{max}$ is nonzero, and for the state variable x_2 only the sensitivity of x_2 to the parameters $K_{12}, K_{-12}, V_{12}^{max}, K_{23}, K_{-23}, V_{23}^{max}$ is nonzero. The vector $S^i = (S_{i1}, \dots, S_{i6}), i = 1, 2$ is used to denote the parametric sensitivity of x_i and $S_n^i = (S_{n1}, \dots, S_{n6})$ is the corresponding normalized sensitivity; for example, $S_{11} = \frac{\partial x_1}{\partial K_{41}}$ denotes the sensitivity of x_1 to K_{41} perturbation and the associate normalized sensitivity $S_{n11} = S_{11}(\frac{K_{41}}{x_1})$. The S_n^i is further visualized as a *single subsystem block* in Simulink environment to perform various perturbation response analysis (see the right-upper and right-down blocks in Fig. 2). In the case of infinitesimal perturbation, we have the following dynamic sensitivity equation of the reversible system, wherein $S_{n1i}, i = 1, \dots, 6$ denote the normalized sensitivity of x_1 to the parameters $K_{41}, K_{-41}, V_{41}^{max}, K_{12}, K_{-12}, V_{12}^{max}$, respectively.

$$\begin{aligned} \frac{dS_{n11}}{dt} &= (A_1^{41} - A_1^{12})S_{n11} + \left(\frac{r_{41}}{b_{41}}\right)\left(\frac{x_4}{K_{41}x_1}\right), \\ \frac{dS_{n12}}{dt} &= (A_1^{41} - A_1^{12})S_{n12} + \left(\frac{r_{41}}{b_{41}}\right)\left(\frac{1}{K_{-41}}\right), \\ \frac{dS_{n13}}{dt} &= (A_1^{41} - A_1^{12})S_{n13} + (r_{41})\left(\frac{1}{x_1}\right), \\ \frac{dS_{n14}}{dt} &= (A_1^{41} - A_2^{12})S_{n14} + A_2^{12}\left(\frac{x_2}{x_1}\right)S_{n21} + \left(\frac{r_{12}}{b_{12}}\right)\left(\frac{1}{K_{12}}\right), \\ \frac{dS_{n15}}{dt} &= (A_1^{41} - A_2^{12})S_{n15} + A_2^{12}\left(\frac{x_2}{x_1}\right)S_{n21} + \left(\frac{r_{12}}{b_{12}}\right)\left(\frac{x_2}{K_{-12}x_1}\right), \\ \frac{dS_{n16}}{dt} &= (A_1^{41} - A_2^{12})S_{n16} + A_2^{12}\left(\frac{x_2}{x_1}\right)S_{n21} + (r_{12})\left(\frac{1}{x_1}\right), \end{aligned} \quad (7)$$

where

$$A_1^{41} \triangleq \frac{\partial r_{41}}{\partial x_1} = -\frac{V_{41}^{max} + \frac{r_{41}}{K_{-41}}}{b_{41}}, A_1^{12} \triangleq \frac{\partial r_{12}}{\partial x_1} = -\frac{V_{12}^{max} - \frac{r_{12}}{K_{12}}}{b_{12}}, A_2^{12} \triangleq \frac{\partial r_{12}}{\partial x_2} = -\frac{V_{12}^{max} + \frac{r_{12}}{K_{-12}}}{b_{12}} \quad \text{and}$$

$$b_{41} = 1 + \frac{x_4}{K_{41}} + \frac{x_1}{K_{-41}}, b_{12} = 1 + \frac{x_1}{K_{12}} + \frac{x_2}{K_{-12}}. \text{ Let } S_{n2i}, i = 1, \dots, 6 \text{ denote the sensitivity of } x_2 \text{ to the parameters } K_{12}, K_{-12}, V_{12}^{max}, K_{23}, K_{-23}, V_{23}^{max}.$$

$$\begin{aligned} \frac{dS_{n21}}{dt} &= A_1^{12}\left(\frac{x_1}{x_2}\right)S_{n14} + (A_2^{12} - A_2^{23})S_{n21} + \left(\frac{r_{12}}{b_{12}}\right)\left(\frac{x_1}{K_{12}x_2}\right), \\ \frac{dS_{n22}}{dt} &= A_1^{12}\left(\frac{x_1}{x_2}\right)S_{n15} + (A_2^{12} - A_2^{23})S_{n22} + \left(\frac{r_{12}}{b_{12}}\right)\left(\frac{1}{K_{-12}}\right), \\ \frac{dS_{n23}}{dt} &= A_1^{12}\left(\frac{x_1}{x_2}\right)S_{n16} + (A_2^{12} - A_2^{23})S_{n23} + (r_{12})\left(\frac{1}{x_2}\right), \\ \frac{dS_{n24}}{dt} &= (A_2^{12} - A_2^{23})S_{n24} + \left(\frac{r_{23}}{b_{23}}\right)\left(\frac{1}{K_{23}}\right), \\ \frac{dS_{n25}}{dt} &= (A_2^{12} - A_2^{23})S_{n25} + \left(\frac{r_{23}}{b_{23}}\right)\left(\frac{x_3}{K_{-23}x_2}\right), \\ \frac{dS_{n26}}{dt} &= (A_2^{12} - A_2^{23})S_{n26} + (r_{23})\left(\frac{1}{x_2}\right), \end{aligned} \quad (8)$$

where $A_2^{23} \triangleq \frac{\partial r_{23}}{\partial x_2} = \frac{V_{23}^{max} - \frac{r_{23}}{K_{23}}}{b_{23}}$ and $b_{23} = 1 + \frac{x_2}{K_{23}} + \frac{x_3}{K_{-23}}$. The differential equations in Eqs. (5), (7) and (8) are further visualized as three individual subsystems (shown in blocks) in Simulink environment. In Fig. 2, the left down subsystem (denoted as \mathbb{S}) is the reversible system in Eq. (5), the right upper subsystem (denoted as S_n^1) describes the dynamic normalized sensitivity of x_1 in Eq. (7) and the right down subsystem (S_n^2) describes the dynamic normalized sensitivity of x_2 in Eq. (8). We use the **Mux** block in Simulink to combine inputs with the same data type and complexity into a vector output (a composite signal), and use **deMux** block to extract and output elements of the composite signal. (See Fig. 3 for the operation of **Mux** block and Fig. 4 for the operation of **deMux** block.) The rb41 denotes a composite signal of the flux r_{41} and the signal b_{41} , The rb12 denotes a composite signal of the flux r_{12} and the signal b_{12} , The rb23 denotes a composite signal of the flux r_{23} and the signal b_{23} , and the A12 denotes a composite signal of two signals A_1^{12} and A_2^{12} . The system \mathbb{S} shares two composite signals rb41 and rb12 with x_1 sensitivity subsystem (denoted as S_n^1), and shares two composite signals rb12 and rb23 with x_2 sensitivity subsystem (denoted as S_n^2). Two sensitivity subsystems share the information of $S_{n14}, S_{n15}, S_{n16}$ and $S_{n21}, S_{n22}, S_{n23}$ because the flux r_{12} possesses three parameters $K_{12}, K_{-12}, V_{12}^{max}$ that

directly effects the dynamic behavior of both x_1 and x_2 . The detailed block diagrams for system \mathbb{S} and sensitivity S_n^1 and S_n^2 are shown in Figs. 3, 4 and 5.

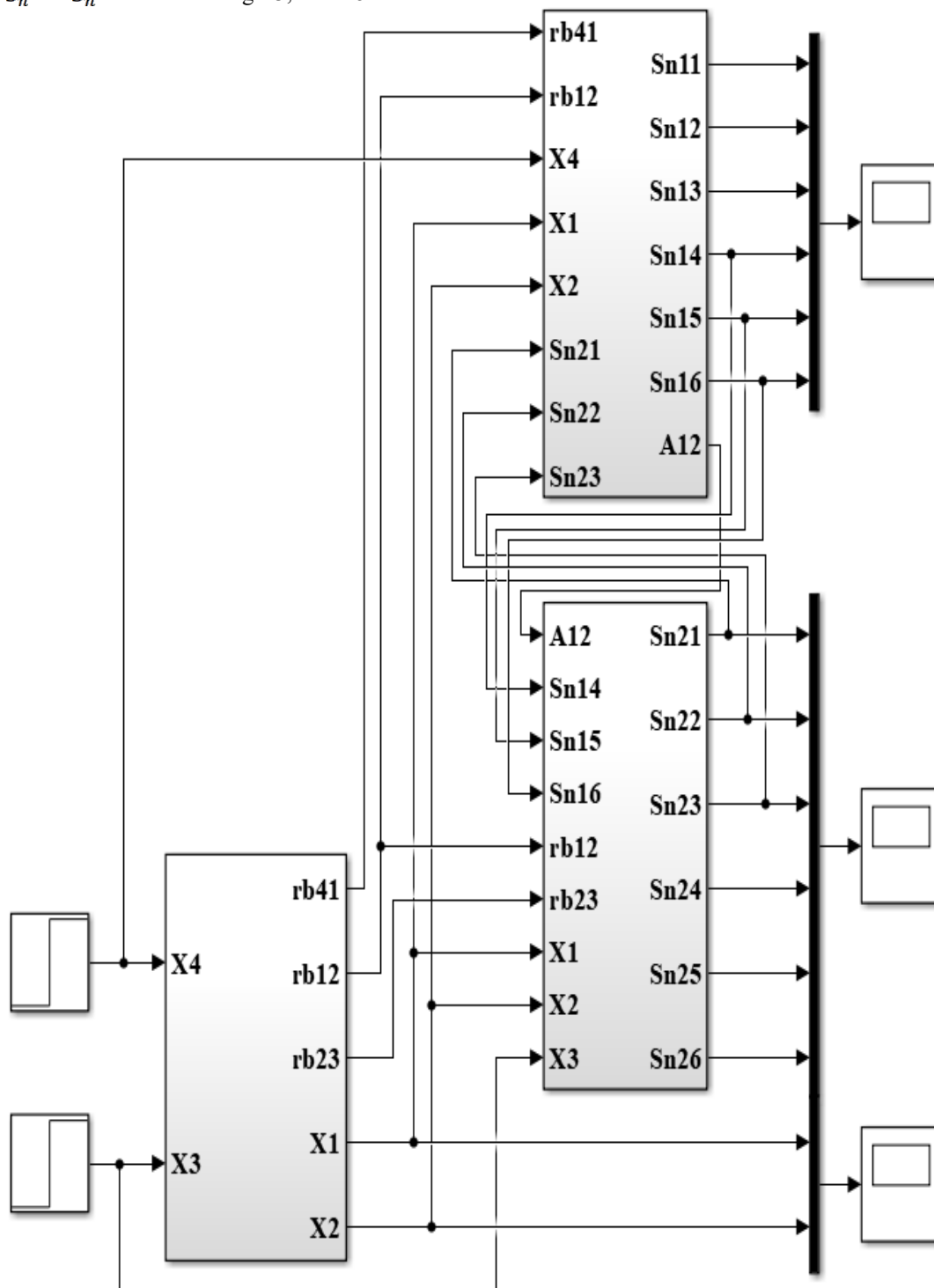


Figure 2: Visualize dynamic behavior and time-varying sensitivity in Simulink environment. The left down block runs the simulation of the reversible system (\mathbb{S}). The right upper block S_n^1 and the right down block S_n^2 are for normalized dynamic sensitivity of x_1 and x_2 , respectively.

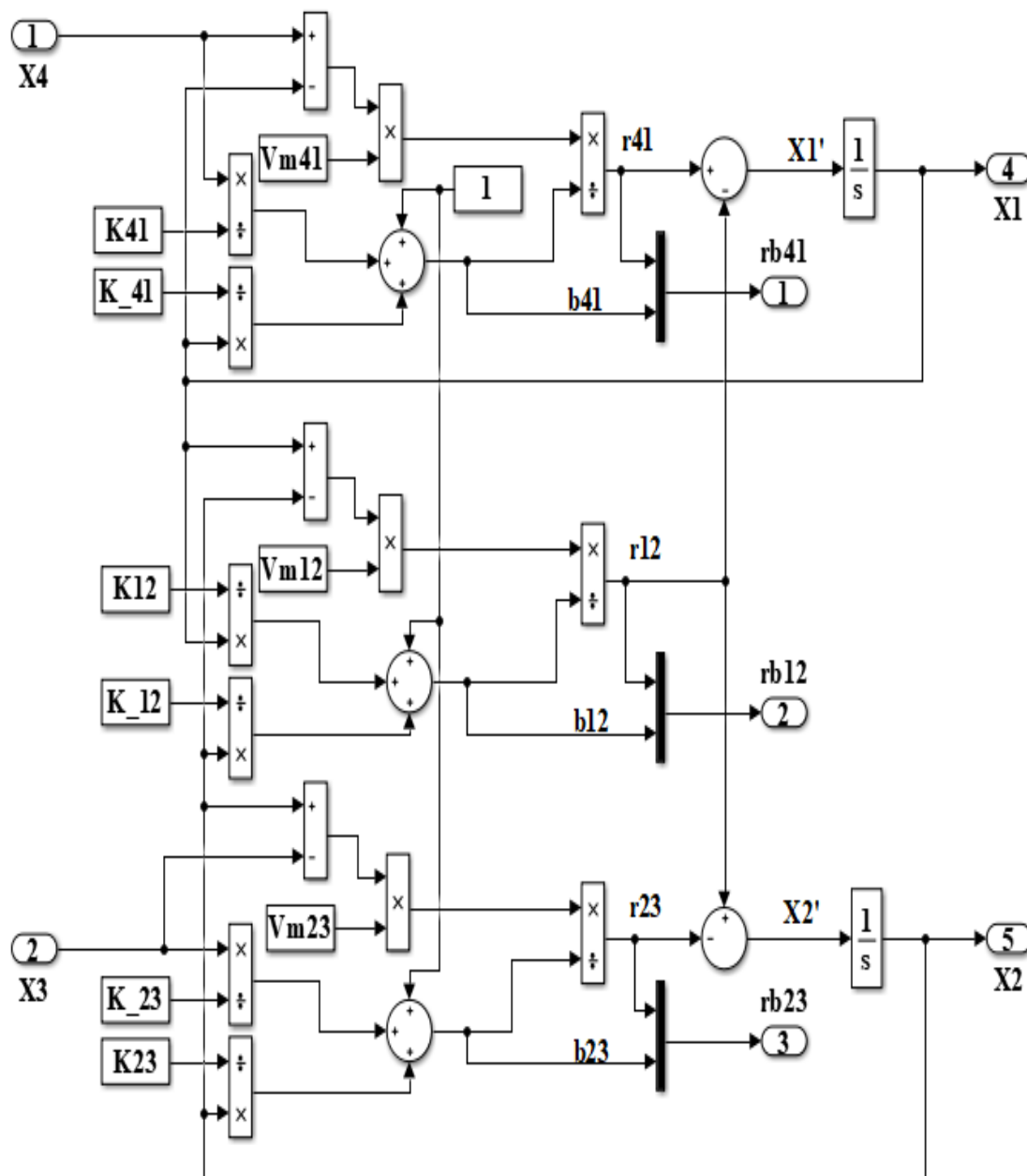


Figure 3: Detailed block diagram for the reversible system S.

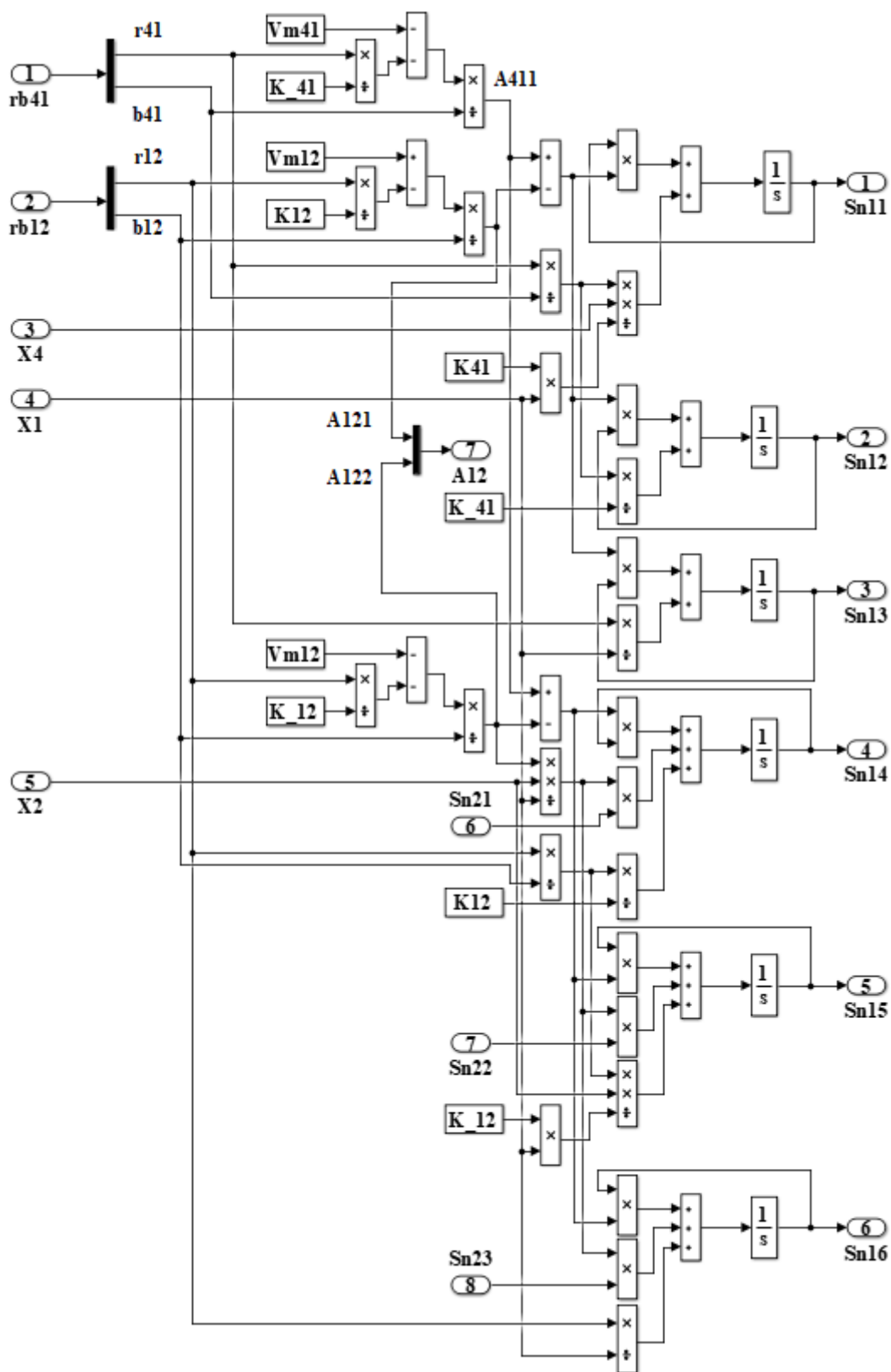


Figure 4: Detailed block diagrams for the dynamic sensitivity of x_1 (right upper block S_n^1)

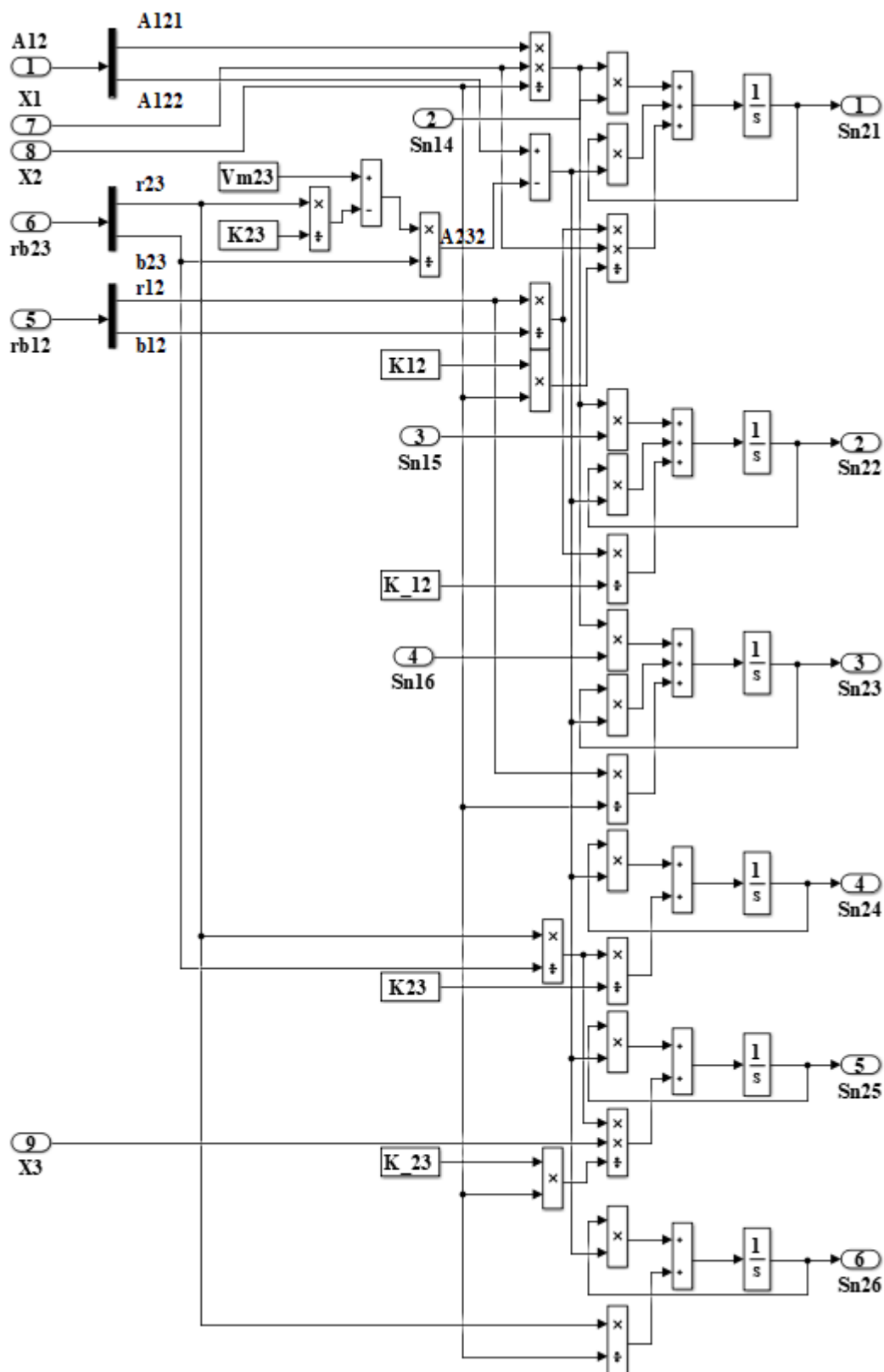


Figure 5: Detailed block diagrams for the dynamic sensitivity of x_2 (right upper block S_n^2).

Dry lab experiments are conducted at an initial condition $(x_{10}, x_{20}) = (4, 3)$ and the independent variable are set at $(x_3, x_4) = (9, 15)$. Figure 6 is the simulation results. The system approaches steady state $(\bar{x}_1, \bar{x}_2) = (12.7126, 10.3047)$. At this dry-lab experimental situation S_{n1i} and S_{n2i} are always positive for $i = 1, \dots, 6$, except in the time period of $t < 0.43$ where in $S_{n24}, S_{n25}, S_{n26} < 0$. (Negative sensitivity means that state variables and parameters go in opposite direction.) The x_1 always shows positive responds to perturbation on the parameters $\{K_{41}, K_{-41}, V_{41}^{max}, K_{23}, K_{-23}, V_{23}^{max}\}$. The x_2 always shows positive responds to the parameters $\{K_{12}, K_{-12}, V_{12}^{max}\}$, but the response of x_2 to the parameters $\{K_{23}, K_{-23}, V_{23}^{max}\}$ is changed from negative to positive at around 0.43 seconds. For parameter perturbation, the influence to x_1 is changed from $S_{n13} > S_{n11} > S_{n16} > S_{n14} > S_{n12} > S_{n15}$ to $S_{n16} > S_{n14} > S_{n13} > S_{n11} > S_{n15} > S_{n12}$ as time goes on (the notation $>$ denotes stronger). The response of x_1 to the perturbations of K_{-41} or K_{-12} is very small. The x_1 has great response to perturbation on V_{41}^{max} and K_{41} at the beginning and on V_{12}^{max} and K_{12} after a period of time (around 0.68 second in this case). The influence of parameter perturbation to x_2 is changed from $S_{n26} > S_{n24} > S_{n25} > S_{n23} > S_{n21} > S_{n22}$ to $S_{n23} > S_{n21} > S_{n26} > S_{n24} > S_{n22} > S_{n25}$ as time goes on. The response of x_2 to the perturbations of K_{-12} or K_{-23} is very small. The x_2 has great response to perturbation on V_{23}^{max} and K_{23} at the beginning and on V_{12}^{max} and K_{12} after a period of time (around 0.47 second in this case). Perturbations on the parameters of reversal reactions (K_{-ij}) have little influence in both x_1 and x_2 . At first the flux r_{41} dominates x_1 and the flux r_{23} dominates x_2 , and later r_{12} dominates both x_1 and x_2 .

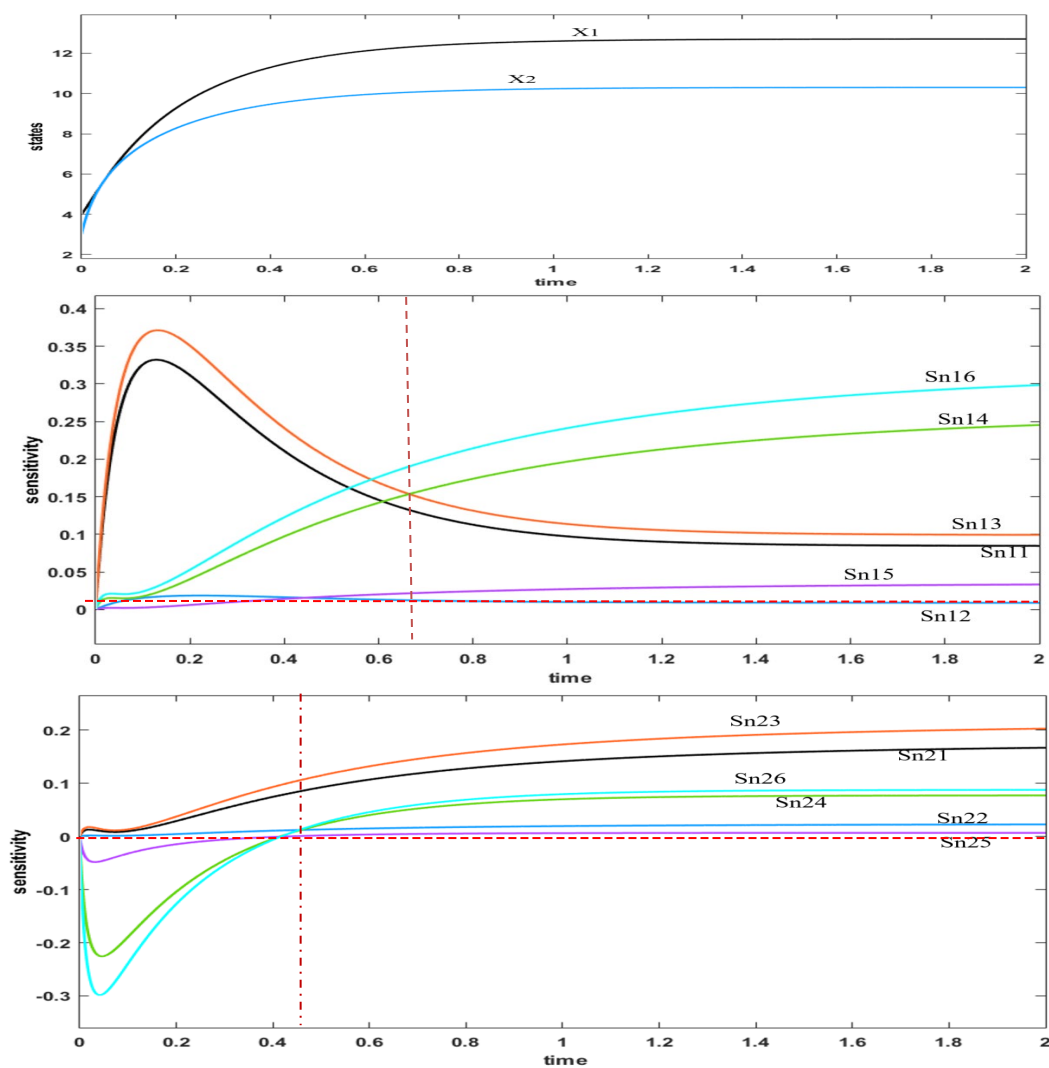


Figure 6: $((x_{10}, x_{20}, x_3, x_4) = (4, 3, 9, 15))$ Simulation results of system dynamic behavior (upper figure), sensitivity of x_1 (middle figure) and sensitivity of x_2 (down figure). $S_{n1i}, i = 1, \dots, 6$ denote the normalized sensitivity of x_1 to the parameters $K_{41}, K_{-41}, V_{41}^{max}, K_{12}, K_{-12}, V_{12}^{max}$ and $S_{n2i}, i = 1, \dots, 6$ denote the sensitivity of x_2 to the parameters $K_{12}, K_{-12}, V_{12}^{max}, K_{23}, K_{-23}, V_{23}^{max}$.

We further conduct an experiment that parameters are perturbed at equilibrium states (a general case for doing sensitivity research.) Simulation results are shown in Fig. 7. We observe $S_{16}^n > S_{14}^n > S_{13}^n > S_{11}^n > S_{15}^n > S_{12}^n$ and $S_{23}^n > S_{21}^n > S_{26}^n > S_{24}^n > S_{22}^n > S_{25}^n$ which is consistency with the results in the final stage for perturbation starting at arbitrary initial conditions. Additionally, we conduct experiments at different independent variables $(x_3, x_4) = (2, 4.8)$ and perturbation starts at (a) an initial condition $(x_{10}, x_{20}) = (14, 10)$ and (b) the steady state. The results are shown in Figs. S1 and S2 of the supplement file. At first the results are different from those mentioned above, but later the ranking results are the same.

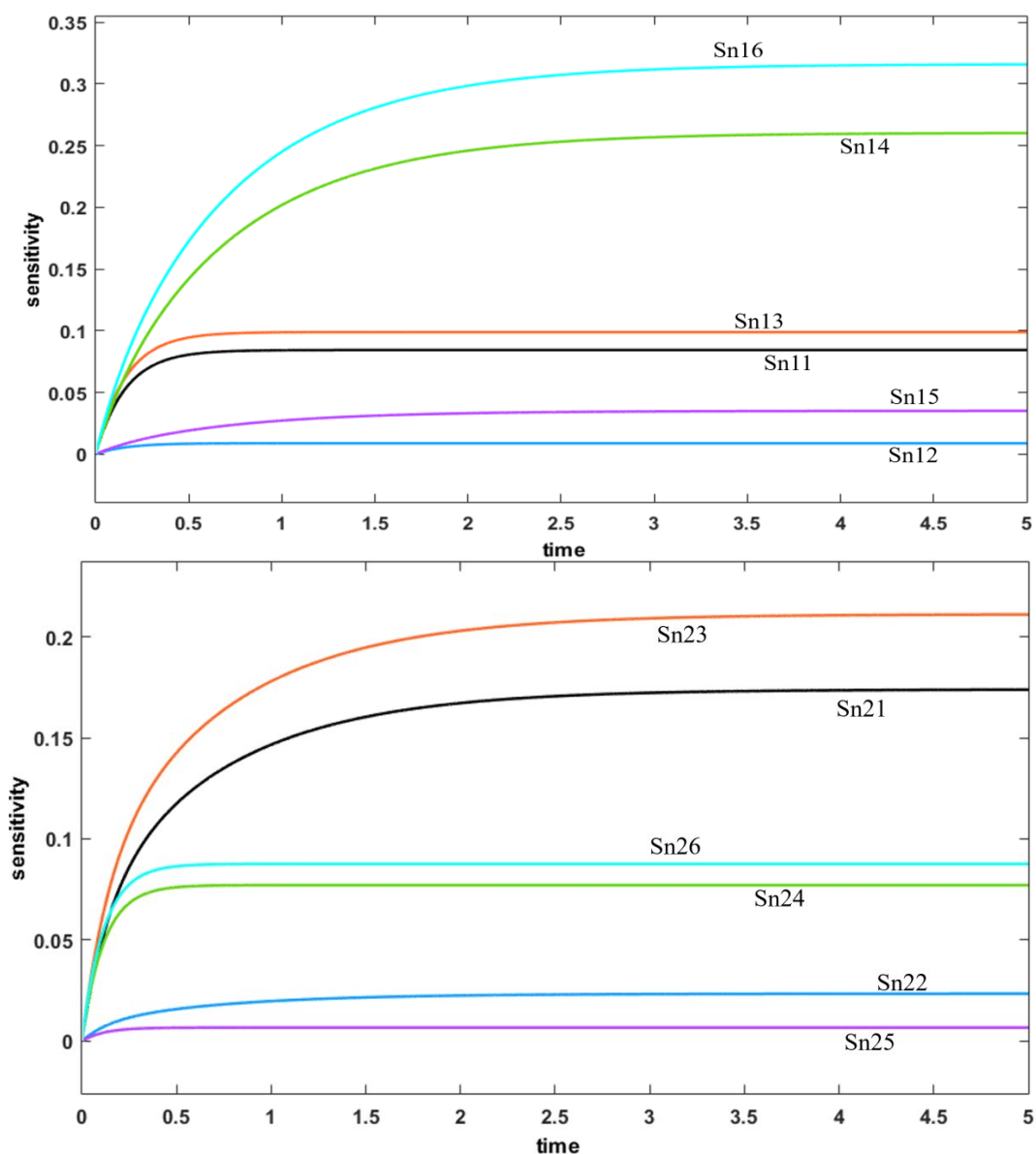


Figure 7: $((x_3, x_4) = (9, 15))$ Perturbation at equilibrium states $(\bar{x}_1, \bar{x}_2) = (12.7109, 10.3036)$. Simulation results of sensitivity of x_1 (upper figure) and sensitivity of x_2 (down figure). $S_{n1i}, i = 1, \dots, 6$ denote the normalized sensitivity of x_1 to the parameters $K_{41}, K_{-41}, V_{41}^{max}, K_{12}, K_{-12}, V_{12}^{max}$ and $S_{n2i}, i = 1, \dots, 6$ denote the sensitivity of x_2 to the parameters $K_{12}, K_{-12}, V_{12}^{max}, K_{23}, K_{-23}, V_{23}^{max}$.

■ Discussion on perturbation response intransient behavior

----- L_2 norm and L_1 norm

Through the above visualization method, we can get time-varying sensitivity for the underlying system being perturbed at any values of state variables. We also observe that the parametric influence ranking near the setting time t_s (the time that takes system transient behavior to decay to a small value) is consistent with that of system being perturbed at equilibrium states. We now further introduce two metrics (L_2 norm and L_1 norm) to get ensemble influence of parameter perturbation to *system transient behavior*. The L_2 norm and L_1 norm for normalized sensitivity $S_{n11}(t)$ in the period of transient state ($t \in [0, t_s]$) are, respectively, defined as $\|S_{n11}\|_2$ in Eq. (9) and IS_{n11} in Eq. (10). The $\|S_{n11}\|_2$ is visualized as the upper figure of Fig. 8 and IS_{n11} as the down figure of Fig. 8.

$$\|S_{n11}\|_2 = \frac{1}{t_s} \sqrt{\int_0^{t_s} |S_{n11}(t)|^2 dt} \quad (9)$$

$$IS_{n11} = \frac{1}{t_s} \int_0^{t_s} |S_{n11}(t)| dt \quad (10)$$

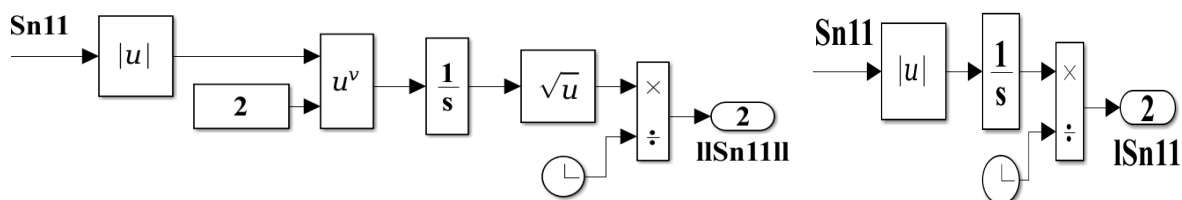


Figure 8: Visualize $\|S_{n11}\|_2$ in Eq. (9) (upper figure) and IS_{n11} in Eq. (10) (down figure) in Simulink.

Figure 9 is the block diagram for the ensemble sensitivity $\|S_{nij}\|$ and Fig. 10 is for the ensemble sensitivity IS_{nij} . Figure 11 shows the detailed block diagrams for the ensemble sensitivity of x_1 (subsystem $\|S_n^1\|$, the right upper block of Fig. 9). An experiment is set at an initial condition $(x_{10}, x_{20}) = (4, 3)$ and the independent variable $(x_3, x_4) = (9, 15)$. The system stabilizes to steady state $(\bar{x}_1, \bar{x}_2) = (12.7126, 10.3047)$ at around 2.7730 (the setting time t_s). Figs. 12 and 13 show the influence of system parameters' perturbation to system transient behavior for these two ensemble sensitivity when the system is conducted at a time period of $[0, t_s]$. We observe that the response of x_1 to parameter perturbation is in the order of $V_{12}^{max} > K_{12} > V_{41}^{max} > K_{41} > K_{-12} > K_{-41}$ and the response of x_2 to parameter perturbation is in the order of $V_{12}^{max} > K_{12} > V_{23}^{max} > K_{23} > K_{-12} > K_{-23}$. The x_1 shows stronger response to variation of the flux v_{12} than to that of the flux v_{41} , and the x_2 shows stronger response to variation of the flux v_{12} than to that of the flux v_{23} . For both x_1 and x_2 , the influence is $V_{ij}^{max} > K_{ij} > K_{-ij}$. We further conducted experiments at various independent variable sets and initial conditions. Tables 1 and 2 show the ensemble sensitivity for various experimental conditions. The influence order is the same as the results mentioned above, except in the case of the initial condition $(x_{10}, x_{20}) = (14, 10)$ and independent variables $(x_3, x_4) = (2, 4, 8)$ wherein the influence order for x_2 is $V_{23}^{max} > K_{12}$ instead of $K_{12} > V_{23}^{max}$ (denoted by pink color in Tables 1 and 2). Looking at the evolution of S_{n2i} , $i = 1, \dots, 6$ for all of the experiments, as shown in the supplement file, we observe that *in this case at the beginning of the experiment* there exists an overshoot for S_{n26} (the sensitivity of x_2 to V_{23}^{max}) which cannot be offset by the subsequent change. Not such a kind of overshoot exists in other sensitivity S_{n2i} , $i = 1, \dots, 5$. Further, in the later experimental process the influence order is the same for all of the experiments. So, the foregoing conclusion is appropriate.

(x_{10}, x_{20})	[4, 3]			[14, 10]		
(x_3, x_4)	[9,15]		[2,4.8]	[9,15]	[2,4.8]	
(x_{1ss}, x_{2ss})	[12.7126,10.3047]			[3.6383,2.5112]	[12.7126,10.3047]	[3.6383 , 2.5112]
t_s	2.7730 (t_s)	3	4	0.7350	2.4490	1.0500
$\ S_{n11}\ $	0.0847	0.0794	0.0632	0.1406	0.0494	0.1186
$\ S_{n12}\ $	0.0067	0.0064	0.0053	0.0135	0.0053	0.0193
$\ S_{n13}\ $	0.0968	0.0908	0.0725	0.1833	0.0579	0.1606
$\ S_{n14}\ $	0.1230	0.1208	0.1113	0.4301	0.1310	0.3545
$\ S_{n15}\ $	0.0168	0.0165	0.0151	0.0495	0.0176	0.0406
$\ S_{n16}\ $	0.1502	0.1473	0.1355	0.5962	0.1589	0.4867
$\ S_{n21}\ $	0.0853	0.0834	0.0760	0.2802	0.0935	0.2345
$\ S_{n22}\ $	0.0116	0.0114	0.0103	0.0322	0.0126	0.0269
$\ S_{n23}\ $	0.1039	0.1016	0.0925	0.3885	0.1134	0.3208
$\ S_{n24}\ $	0.0492	0.0471	0.0402	0.1446	0.0482	0.2222
$\ S_{n25}\ $	0.0065	0.0061	0.0049	0.0113	0.0042	0.0113
$\ S_{n26}\ $	0.0586	0.0559	0.0473	0.1841	0.0547	0.2590

Table 1: (L_2 norm) the influence of system parameters' perturbation to the transient behavior. $\|S_{n1i}\|, i = 1, \dots, 6$ denote the ensemble sensitivity of x_1 to the parameters $K_{41}, K_{-41}, V_{41}^{max}, K_{12}, K_{-12}, V_{12}^{max}$ and $\|S_{n2i}\|, i = 1, \dots, 6$ denote the ensemble sensitivity of x_2 to the parameters $K_{12}, K_{-12}, V_{12}^{max}, K_{23}, K_{-23}, V_{23}^{max}$.

(x_{10}, x_{20})	[4, 3]			[14, 10]		
(x_3, x_4)	[9,15]		[2,4.8]	[9,15]	[2,4.8]	
(x_{1ss}, x_{2ss})	[12.7126,10.3047]			[3.6383,2.5112]	[12.7126,10.3047]	[3.6383 , 2.5112]
t_s	2.7730 (t_s)	3	4	0.7350	2.4490	1.0500
IS_{n11}	0.1231	0.1202	0.1112	0.1168	0.0750	0.1146
IS_{n12}	0.0108	0.0106	0.0102	0.0112	0.0080	0.0160
IS_{n13}	0.1421	0.1388	0.1289	0.1523	0.0880	0.1544
IS_{n14}	0.1919	0.1967	0.2121	0.3394	0.1960	0.3189
IS_{n15}	0.0263	0.0269	0.0289	0.0391	0.0263	0.0366
IS_{n16}	0.2348	0.2405	0.2588	0.4702	0.2375	0.4350
IS_{n21}	0.1338	0.1366	0.1457	0.2291	0.1428	0.2255
IS_{n22}	0.0183	0.0187	0.0199	0.0264	0.0191	0.0260
IS_{n23}	0.1634	0.1668	0.1776	0.3174	0.1730	0.3064
IS_{n24}	0.0744	0.0746	0.0752	0.1229	0.0744	0.1953
IS_{n25}	0.0079	0.0078	0.0075	0.0096	0.0065	0.0110
IS_{n26}	0.0866	0.0867	0.0869	0.1565	0.0845	0.2338

Table 2: (L_1 norm) the influence of system parameters' perturbation to the transient behavior. $IS_{n1i}, i = 1, \dots, 6$ denote the ensemble sensitivity of x_1 to the parameters $K_{41}, K_{-41}, V_{41}^{max}, K_{12}, K_{-12}, V_{12}^{max}$ and $IS_{n2i}, i = 1, \dots, 6$ denote the ensemble sensitivity of x_2 to the parameters $K_{12}, K_{-12}, V_{12}^{max}, K_{23}, K_{-23}, V_{23}^{max}$.

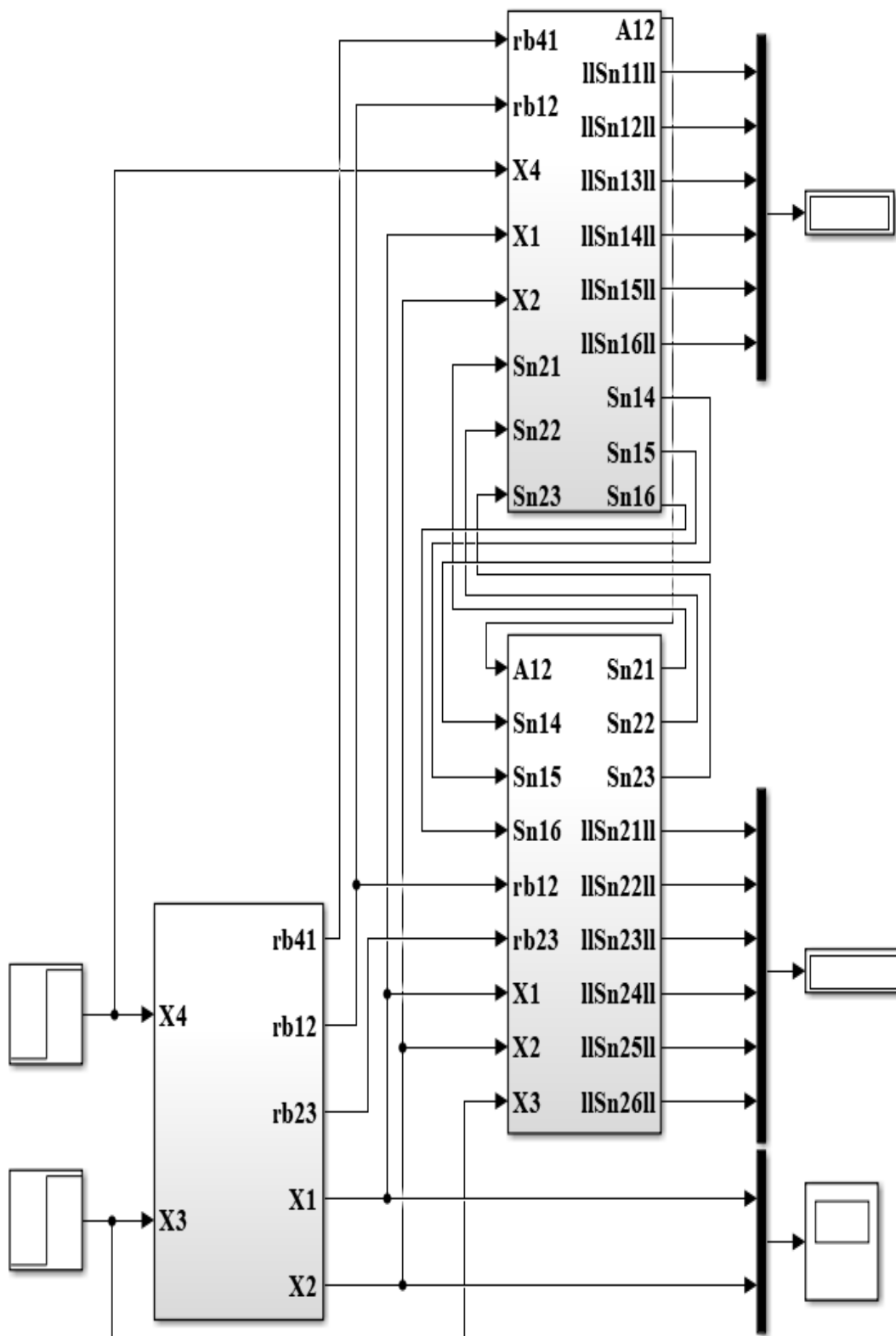


Figure 9: Visualize dynamic behavior and ensemble sensitivity $\|S_{nij}\|_2$ in Simulink environment. The left down block runs the simulation of the reversible system (S). The right upper block $\|S_n^1\|$ and the right down block $\|S_n^2\|$ are for normalized ensemble sensitivity of x_1 and x_2 , respectively.

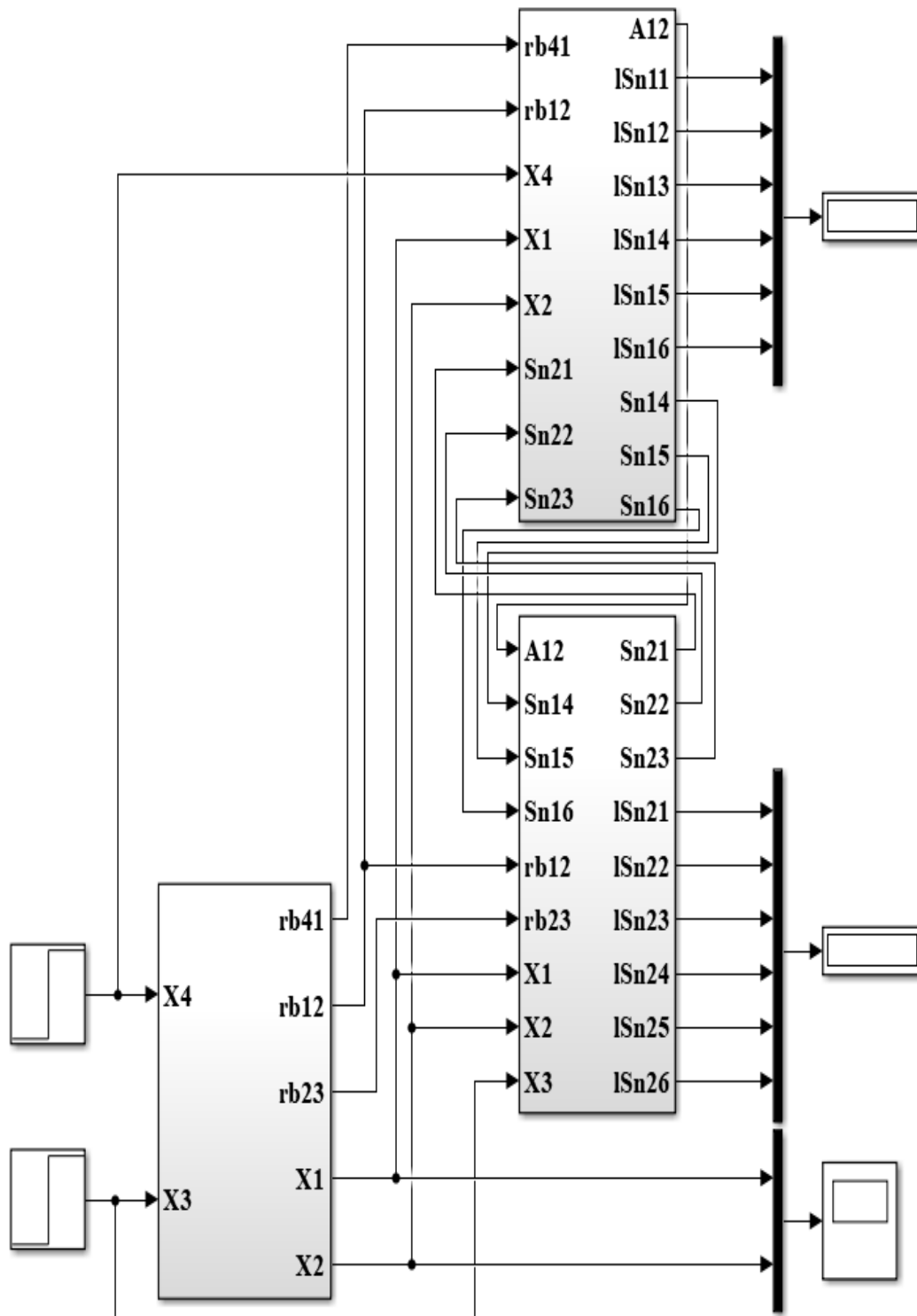


Figure 10: Visualize dynamic behavior and ensemble sensitivity $IS_{n,j}$ in Simulink environment. The left down block runs the simulation of the reversible system (S). The right upper block IS_n^1 and the right down block IS_n^2 are for normalized ensemble sensitivity of x_1 and x_2 , respectively.

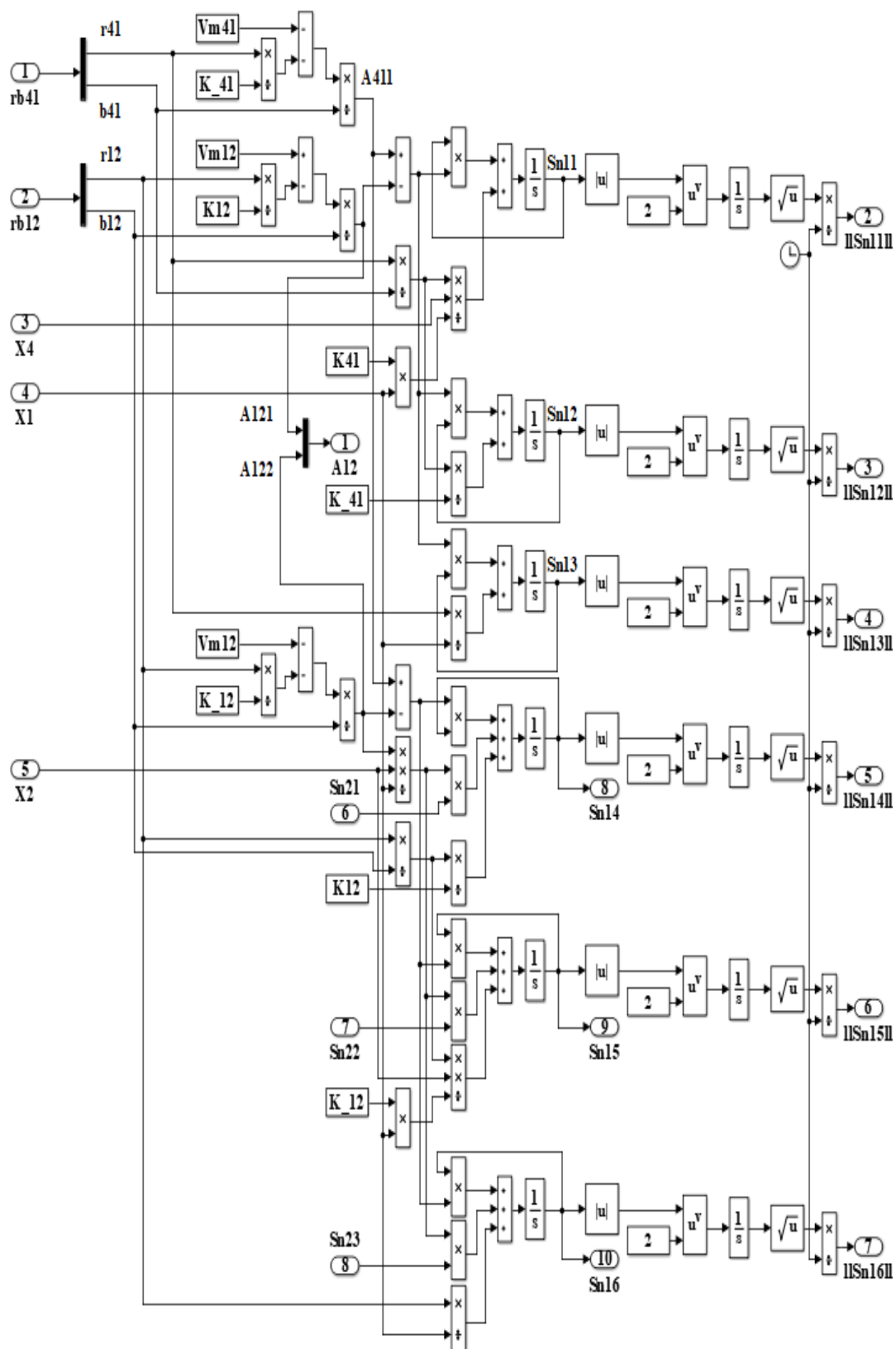


Figure 11: Detailed block diagrams for the ensemble sensitivity of x_1 (right upper block $||S_n^1||$).

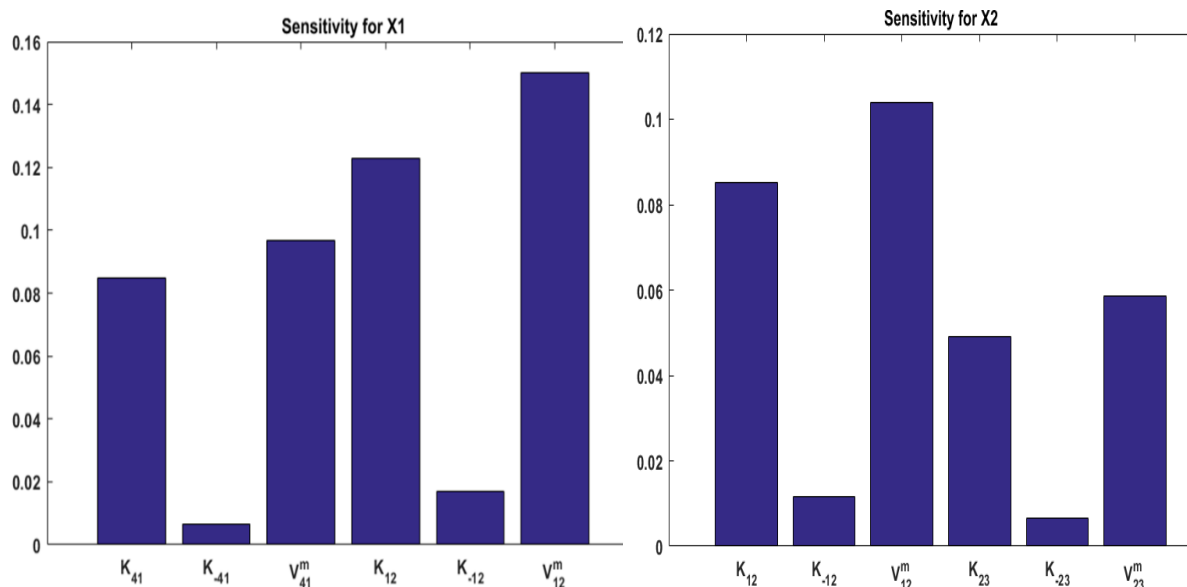


Figure 12: (L_2 norm) the influence of system parameters' perturbation to system transient behavior for initial condition $(x_{10}, x_{20}) = (4, 3)$ and independent variable $(x_3, x_4) = (9, 15)$.

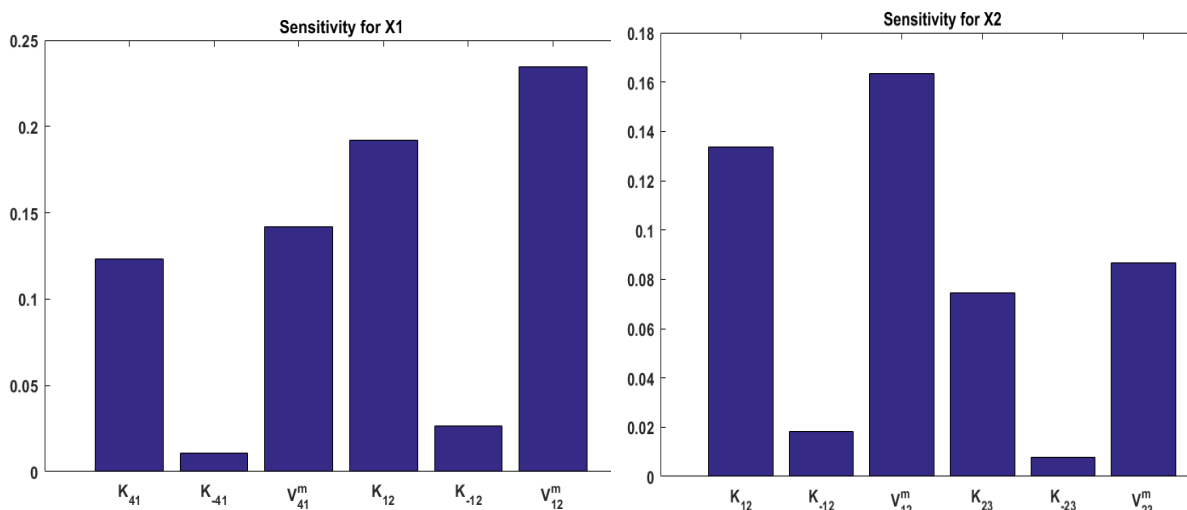


Figure 13: (L_1 norm) the influence of system parameters' perturbation to system transient behavior for initial condition $(x_{10}, x_{20}) = (4, 3)$ and independent variable $(x_3, x_4) = (9, 15)$.

■ Results and discussion on the perturbation response in steady states

----- independent variable perturbation and parametric perturbation

When the three net fluxes of the system are equal ($r_{41} = r_{12} = r_{23}$) the system reaches equilibrium and the steady states are $\bar{x}_1 = \frac{\bar{r} + (V_{41}^{max} + \frac{\bar{r}}{K_{41}})x_4}{V_{41}^{max} - \frac{\bar{r}}{K_{-41}}}$ and $\bar{x}_2 = \frac{(V_{23}^{max} - \frac{\bar{r}}{K_{-23}})x_3 - \bar{r}}{V_{23}^{max} + \frac{\bar{r}}{K_{23}}}$, where \bar{r} is the constant net flux at equilibrium,

$\bar{r} = \bar{r}_{41} = \bar{r}_{12} = \bar{r}_{23}$. Both steady states, \bar{x}_1 and \bar{x}_2 , response to only three parametric perturbations. The static sensitivity of \bar{x}_1 to the parameters $K_{41}, K_{-41}, V_{41}^{max}$ are denoted as $\bar{S}_{11}, \bar{S}_{12}, \bar{S}_{13}$:

$$\bar{S}_{11} = -\frac{\bar{r}x_4K_{41}^{-2}}{V_{41}^{max} - \frac{\bar{r}}{K_{-41}}},$$

$$\bar{S}_{12} = -\frac{\bar{r}\bar{x}_1K_{-41}^{-2}}{V_{41}^{max} - \frac{\bar{r}}{K_{-41}}},$$

$$\bar{S}_{13} = \frac{x_4 + \bar{x}_1}{V_{41}^{max} - \frac{\bar{r}}{K_{-41}}}.$$

The static sensitivity of \bar{x}_2 to the parameters $K_{23}, K_{-23}, V_{23}^{max}$ are denoted as $\bar{S}_{24}, \bar{S}_{25}, \bar{S}_{26}$:

$$\bar{S}_{24} = \frac{\bar{r}\bar{x}_2 K_{23}^{-2}}{V_{23}^{max} + \frac{\bar{r}}{K_{23}}},$$

$$\bar{S}_{25} = \frac{\bar{r}\bar{x}_3 K_{-23}^{-2}}{V_{23}^{max} + \frac{\bar{r}}{K_{23}}},$$

$$\bar{S}_{26} = \frac{\bar{x}_3 - \bar{x}_2}{V_{23}^{max} + \frac{\bar{r}}{K_{23}}}.$$

The normalized static sensitivities are $\bar{S}_{n11} = \bar{S}_{11} \left(\frac{K_{41}}{\bar{x}_1} \right), \bar{S}_{n12} = \bar{S}_{12} \left(\frac{K_{-41}}{\bar{x}_1} \right), \bar{S}_{n13} = \bar{S}_{13} \left(\frac{V_{41}^{max}}{\bar{x}_1} \right); \bar{S}_{n24} = \bar{S}_{24} \left(\frac{K_{23}}{\bar{x}_2} \right), \bar{S}_{n25} = \bar{S}_{25} \left(\frac{K_{-23}}{\bar{x}_2} \right), \bar{S}_{n26} = \bar{S}_{26} \left(\frac{V_{23}^{max}}{\bar{x}_2} \right)$

We now set an experiment that is conducted at a fixed independent variable and let another independent variable vary from 0 to infinity. An infinity x_4 (or x_3) denotes that the quantity of x_4 is extremely large compared to that of other constituents, instead of the concentration of x_4 being infinity. *The infinity value is to find out the limiting influence strength.* Tables 3 and 4, respectively, show the static sensitivity for the cases of the fixed independent variable $x_3 = 1$ and $x_3 = 10$. (The values for time-varying independent variables are cited from our previously paper using the **rlocus** command in Matlab toolbox [29].) Tables 5 and 6, respectively, are the static sensitivity for the cases of the fixed independent variable $x_4 = 4.8$ and $x_4 = 15$.

For the case of $x_3 = 1$, the reversible pathway is in a favorable direction of $x_4 \rightarrow x_3$ when the gain is $x_4 > 1$, in which the net flux \bar{r} is negative. For the case of $x_3 = 10$, the reversible pathway is in a favorable direction of $x_4 \rightarrow x_3$ when the gain is $x_4 > 10$. The reversal point of netflux direction locates exactly at the experimental condition that the value of varying independent variable equals to that of the fixed independent variable ($x_4 = 1$ for fixed $x_3 = 1$ in Table 3 and $x_4 = 10$ for fixed $x_3 = 10$ in Table 4, and $x_3 = 4.8$ for fixed $x_4 = 4.8$ in Table 5 and $x_3 = 15$ for fixed $x_4 = 15$ in Table 6.) For clarity, we denote the results for the case of $\bar{r} > 0$ by **olive green**. We observe that (a) when x_3 is fixed the net flux \bar{r} has the same sign with $\bar{S}_{n2i}, i = 1, \dots, 3$ but opposite sign with \bar{S}_{n12} and \bar{S}_{n13} ($\bar{r} > 0, \bar{S}_{n12} < 0, \bar{S}_{n13} < 0, \bar{S}_{n2i} > 0, i = 1, \dots, 3$ and $\bar{r} < 0, \bar{S}_{n12} > 0, \bar{S}_{n13} > 0, \bar{S}_{n2i} < 0, i = 1, \dots, 3$.) The \bar{S}_{n11} is always negative except some points which are noted with pink color. (b) When x_4 is fixed the net flux \bar{r} has the same sign with $\bar{S}_{n1i}, i = 1, \dots, 3$ but opposite sign with $\bar{S}_{n2i}, i = 1, \dots, 3$, except two points in \bar{S}_{n11} . ($\bar{S}_{n11} = \frac{\partial x_1/x_1}{\partial K_{41}/K_{41}} < 0$ denoted that x_1 decreases as K_{41} increases.)

At the case of fixed x_3 , when the system is in the favorable direction ($x_4 \rightarrow x_3, \bar{r} < 0$) the \bar{x}_1 always shows negative response to K_{41} perturbation, but positive response to V_{41}^{max} and K_{-41} . The \bar{x}_2 shows negative response to perturbations of V_{23}^{max}, K_{23} and K_{-23} . At the case of fixed x_4 , when the system is in the favorable direction ($x_4 \rightarrow x_3, \bar{r} < 0$) the \bar{x}_1 shows negative response to perturbations K_{41}, V_{41}^{max} and K_{-41} . The \bar{x}_2 shows positive response to perturbations of V_{23}^{max}, K_{23} and K_{-23} .

For a given independent variable set (x_3, x_4), the \bar{x}_1 shows great response to V_{41}^{max} than to K_{-41} and the ranking for the response of \bar{x}_2 to parameter perturbation is $V_{23}^{max} > K_{23} > K_{-23}$. The reaction reverse point $\bar{r} = 0$ (the point for $x_3 = x_4$) is a branch point. Except the sensitivity \bar{S}_{n11} , the absolutely normalized sensitivity $|\bar{S}_{nij}|$ becomes larger and larger as the varying independent variable gets bigger and bigger or smaller and smaller (the minimum $|\bar{S}_{nij}|$ exists at $\bar{r} = 0$). At fixed x_3 the maximum sensitivity $\text{Max}_{x_4} (|\bar{S}_{n11}|, |\bar{S}_{n12}|, |\bar{S}_{n13}|, |\bar{S}_{n24}|, |\bar{S}_{n25}|, |\bar{S}_{n26}|) = (1.4527, 0.0924, 4.5005, 2.5000, 0.0500, 2.8000)$ for $x_3 = 1$, and $(8.3766, 0.0925, 4.5088, 2.5000, 0.0645, 2.5968)$ for $x_3 = 10$. At fixed x_4 the maximum sensitivity $\text{Max}_{x_3} (|\bar{S}_{n11}|, |\bar{S}_{n12}|, |\bar{S}_{n13}|, |\bar{S}_{n24}|, |\bar{S}_{n25}|, |\bar{S}_{n26}|) = (13.4632, 1.6667, 2.5247, 0.8080, 0.7264, 1.5343)$ for $x_4 = 4.8$, and $(15.1310, 1.6667, 2.5088, 0.8080, 0.7263, 1.5343)$ for $x_4 = 15$. These maximal values are marked in bold letters.

x_4	\bar{S}_{n11}	\bar{S}_{n12}	\bar{S}_{n13}	\bar{S}_{n24}	\bar{S}_{n25}	\bar{S}_{n26}
	(K_{41})	(K_{-41})	(V_{41}^{max})	(K_{23})	(K_{-23})	(V_{23}^{max})
0	0	-0.03382909	-1.03382909	0.183260294	0.025928773	0.33883293
0.057602429	-0.02914142	-0.030622	-0.8442013	0.169256155	0.023211525	0.308525306
0.180882237	-0.06008395	-0.02458778	-0.58080321	0.141303541	0.018258292	0.250853295
0.568003538	-0.05762235	-1.06E-02	-0.19822479	0.066925407	0.007495123	0.111896147
1.783635726	0.15444959	0.012595316	0.202025435	-0.09585389	-0.00831079	-0.14571865
5.600944689	1.452711341	0.038229349	0.637630511	-0.37469148	-0.02342544	-0.51524414
17.58799791	-128.527304	0.059318084	1.201339913	-0.76180974	-0.03433283	-0.96780674
55.22955279	-7.06694553	0.074184109	1.952987715	-1.21951745	-0.04132237	-1.46745169
173.430968	-6.52662454	0.083808021	2.871886642	-1.68278019	-0.04557356	-1.95622155
544.605182	-7.10674674	0.089498739	3.802319728	-2.06777184	-0.04799357	-2.35573327
882.0079451	-7.38701015	0.091001404	4.136453661	-2.18959218	-0.04862144	-2.48132079
1219.410708	-7.55795882	0.091776441	4.329213249	-2.25645581	-0.04894348	-2.55011672
1220.63134	-7.55845682	0.091778575	4.329765647	-2.25664402	-0.04894437	-2.55031024
1221.851971	-7.55895412	0.091780706	4.330317224	-2.25683192	-0.04894525	-2.55050344
1710.160577	-7.71439262	0.092416577	4.500542032	-2.3139236	-0.04920857	-2.60917501
inf	-	-	-	-2.5000000	-0.05000000	-2.80000000

Table 3: ($x_3 = 1$) Static sensitivity for perturbation from independent variables and parameters.

x_4	\bar{S}_{n11}	\bar{S}_{n12}	\bar{S}_{n13}	\bar{S}_{n24}	\bar{S}_{n25}	\bar{S}_{n26}
	(K_{41})	(K_{-41})	(V_{41}^{max})	(K_{23})	(K_{-23})	(V_{23}^{max})
0.0000	0.0000	-0.1436	-1.1436	0.4627	0.0989	0.6110
0.1542	-0.0363	-0.1304	-1.0040	0.4417	0.0898	0.5763
0.5391	-0.0857	-0.1065	-0.7937	0.3975	0.0732	0.5074
1.8849	-0.1327	-0.0634	-0.4855	0.2903	0.0436	0.3556
6.5903	-0.0815	-0.0146	-0.1318	0.0899	0.0100	0.1049
23.0421	0.4614	0.0252	0.3004	-0.2155	-0.0173	-0.2414
80.5636	8.3766	0.0531	0.8840	-0.6240	-0.0363	-0.6785
281.6799	-7.5390	0.0713	1.6800	-1.1128	-0.0488	-1.1860
984.8555	-6.3925	0.0827	2.6838	-1.6212	-0.0566	-1.7061
3443.4138	-7.0285	0.0893	3.7295	-2.0509	-0.0611	-2.1425
6050.4829	-7.3695	0.0911	4.1294	-2.1939	-0.0623	-2.2874
8657.5520	-7.5625	0.0919	4.3430	-2.2662	-0.0628	-2.3605
8666.2182	-7.5630	0.0919	4.3436	-2.2664	-0.0628	-2.3606
8674.8844	-7.5635	0.0919	4.3441	-2.2666	-0.0628	-2.3608
12039.4303	-7.7163	0.0925	4.5088	-2.3204	-0.0633	-2.4153
inf	-	-	-	-2.5000	-0.0645	-2.5968

Table 4: ($x_3 = 10$) Static sensitivity for perturbation from independent variables and parameters.

x_3	\bar{S}_{n11}	\bar{S}_{n12}	\bar{S}_{n13}	\bar{S}_{n24}	\bar{S}_{n25}	\bar{S}_{n26}
	(K_{41})	(K_{-41})	(V_{41}^{max})	(K_{23})	(K_{-23})	(V_{23}^{max})
0.0000	13.4632	0.0543	1.3023	-0.6496	0.0000	-1.6496
0.2057	5.0236	0.0491	1.0477	-0.5490	-0.0187	-1.0219
0.9935	1.1065	0.0350	0.5758	-0.3315	-0.0216	-0.4620
4.7999	0.0000	0.0000	0.0000	0.0000	0.0000	0.0000
23.1891	-0.1462	-0.0671	-0.4451	0.3013	0.0455	0.3566
67.6093	-0.1333	-0.1387	-0.6795	0.4552	0.0918	0.5537
112.0296	-0.1209	-0.1822	-0.7805	0.5138	0.1188	0.6379
219.3294	-0.1035	-0.2516	-0.9118	0.5796	0.1605	0.7437
326.6292	-0.0937	-0.2999	-0.9903	0.6127	0.1885	0.8040
433.9290	-0.0871	-0.3378	-1.0472	0.6339	0.2099	0.8463
541.2288	-0.0821	-0.3695	-1.0924	0.6492	0.2275	0.8788
800.4182	-0.0740	-0.4306	-1.1748	0.6736	0.2605	0.9357

1059.6076	-0.0687	-0.4783	-1.2361	0.6893	0.2855	0.9762
1318.7970	-0.0648	-0.5179	-1.2853	0.7006	0.3058	1.0075
1577.9864	-0.0617	-0.5520	-1.3267	0.7092	0.3229	1.0331
2096.3651	-0.0573	-0.6087	-1.3940	0.7218	0.3507	1.0733
2614.7439	-0.0540	-0.6553	-1.4481	0.7308	0.3729	1.1044
3240.8321	-0.0511	-0.7023	-1.5019	0.7388	0.3948	1.1342
3866.9202	-0.0489	-0.7424	-1.5470	0.7450	0.4130	1.1585
5119.0965	-0.0456	-0.8083	-1.6203	0.7540	0.4422	1.1966
6371.2728	-0.0432	-0.8612	-1.6785	0.7604	0.4649	1.2257
7623.4491	-0.0415	-0.9055	-1.7268	0.7652	0.4835	1.2490
12632.1543	-0.0371	-1.0324	-1.8632	0.7769	0.5346	1.3118
15656.8643	-0.0355	-1.0864	-1.9207	0.7812	0.5554	1.3368
18681.5744	-0.0343	-1.1303	-1.9672	0.7844	0.5720	1.3566
24730.9944	-0.0325	-1.1984	-2.0389	0.7889	0.5970	1.3861
36829.8346	-0.0305	-1.2897	-2.1345	0.7943	0.6293	1.4238
61027.5148	-0.0285	-1.3919	-2.2409	0.7996	0.6640	1.4637
136811.2948	-0.0264	-1.5154	-2.3688	0.8051	0.7039	1.5090
212595.0747	-0.0257	-1.5618	-2.4167	0.8070	0.7184	1.5253
212807.8826	-0.0257	-1.5619	-2.4168	0.8070	0.7184	1.5254
213020.6905	-0.0257	-1.5620	-2.4169	0.8070	0.7184	1.5254
294831.5447	-0.0253	-1.5879	-2.4436	0.8080	0.7264	1.5343
inf	-0.0242	-1.6667	-2.5247	-	-	-

Table 5: ($x_4 = 4.8$) Static sensitivity for perturbation from independent variables and parameters.

x_3	\bar{S}_{n11}	\bar{S}_{n12}	\bar{S}_{n13}	\bar{S}_{n24}	\bar{S}_{n25}	\bar{S}_{n26}
	(K_{41})	(K_{-41})	(V_{41}^{max})	(K_{23})	(K_{-23})	(V_{23}^{max})
0.0000	-8.6610	0.0705	1.9061	-1.0841	0.0000	-2.0841
0.4011	-15.1310	0.0639	1.4597	-0.8803	-0.0287	-1.2669
2.0167	3.8085	0.0479	0.8008	-0.5271	-0.0308	-0.6343
10.1395	0.1446	0.0125	0.1339	-0.0953	-0.0086	-0.1081
50.9790	-0.1478	-0.0523	-0.3502	0.2542	0.0354	0.2931
153.6447	-0.1469	-0.1217	-0.6025	0.4266	0.0806	0.5099
256.3103	-0.1353	-0.1632	-0.7082	0.4904	0.1067	0.5992
514.3992	-0.1170	-0.2315	-0.8474	0.5631	0.1482	0.7127
772.4881	-0.1063	-0.2784	-0.9286	0.5989	0.1758	0.7758
1288.6660	-0.0936	-0.3460	-1.0328	0.6380	0.2141	0.8530
1613.0682	-0.0883	-0.3788	-1.0798	0.6532	0.2323	0.8862
1937.4703	-0.0842	-0.4071	-1.1188	0.6649	0.2477	0.9132
2586.2747	-0.0781	-0.4546	-1.1819	0.6818	0.2729	0.9553
3235.0790	-0.0737	-0.4939	-1.2322	0.6939	0.2933	0.9876
3883.8833	-0.0702	-0.5275	-1.2742	0.7031	0.3104	1.0139
5181.4920	-0.0651	-0.5836	-1.3424	0.7165	0.3383	1.0551
6479.1007	-0.0615	-0.6296	-1.3968	0.7260	0.3605	1.0867
8110.1163	-0.0580	-0.6778	-1.4529	0.7348	0.3832	1.1182
9741.1318	-0.0554	-0.7186	-1.4997	0.7414	0.4021	1.1437
13003.1630	-0.0516	-0.7855	-1.5752	0.7510	0.4321	1.1833
16265.1942	-0.0489	-0.8391	-1.6348	0.7578	0.4554	1.2133
19527.2253	-0.0468	-0.8839	-1.6841	0.7629	0.4744	1.2374
32575.3500	-0.0418	-1.0122	-1.8232	0.7752	0.5266	1.3019
40775.7015	-0.0399	-1.0687	-1.8838	0.7799	0.5486	1.3285
48976.0531	-0.0385	-1.1145	-1.9326	0.7833	0.5660	1.3494
65376.7563	-0.0365	-1.1852	-2.0075	0.7881	0.5922	1.3803
98178.1626	-0.0341	-1.2793	-2.1066	0.7938	0.6257	1.4195
163780.9752	-0.0318	-1.3844	-2.2165	0.7992	0.6615	1.4608

378775.4276	-0.0293	-1.5143	-2.3514	0.8051	0.7035	1.5086
593769.8799	-0.0285	-1.5618	-2.4005	0.8070	0.7183	1.5253
594364.2442	-0.0285	-1.5618	-2.4006	0.8070	0.7184	1.5253
594958.6084	-0.0285	-1.5619	-2.4007	0.8070	0.7184	1.5254
823451.1016	-0.0281	-1.5879	-2.4275	0.8080	0.7263	1.5343
inf	-0.0269	-1.6667	-2.5088	-	-	-

Table 6: ($\mathbf{x}_4 = \mathbf{15}$)Static sensitivity for perturbation from independent variables and parameters.

IV. CONCLUSION

A constitute (genes, proteins, metabolites), in fact, physically interacts with about four ingredients at most. Most of elements of the sensitivity matrix S are zero. So, system parameters can be decomposed into several groups and perturb these groups one by one. In this study, we further visualize the reduced normalized dynamic sensitivity equations and system equations as integrated blocks denoting subsystems in the block-diagrams-based Simulink environment. In this way, the difficulty in simultaneously solving system equations and sensitivity equations is largely reduced. The proposed approach is able to find out the dynamic sensitivity of various biological or physical systems. Additionally, the normalized *dynamic* sensitivity curves are affected by initial states of the underlying systems. So, two ensemble metrics, L_2 norm and L_1 norm, is introduced to get parametric influence ranking on *system transient behavior*. We further discuss the normalized *static* sensitivity of systems for perturbations from independent variables or parameters. The tendency of system steady states to independent variable variations, the parametric influence ranking and the limiting influence strength for various parameter perturbations are sufficiently discussed. In the future, we shall develop controllers to let biological systems possess satisfactory dynamic behavior.

ACKNOWLEDGMENT

This research was supported by grant number MOST 109-2221-E-212-003 from the Ministry of Science and Technology of Taiwan, R.O.C.

REFERNCES

- [1]. Voit EO (2013) Biochemical systems theory: a review. ISRN Biomathematics. <https://doi.org/10.1155/2013/897658>
- [2]. Sriyudthsak K, Shiraiishi F, Hirai MY (2016) Mathematical modeling and dynamic simulation of metabolic reaction systems using metabolome time series data. Front Mol Biosci. <https://doi.org/10.3389/fmolb.2016.00015>
- [3]. Bartocci E, Lió P (2016) Computational Modeling, Formal Analysis, and Tools for Systems Biology. PLoS Comput Biol. <https://doi.org/10.1371/journal.pcbi.1004591>
- [4]. Wu SJ, Wu CT, Chang JY (2013) Adaptive neural-based fuzzy modeling for biological systems. Math Biosci 242(2):153-60
- [5]. Liu S, Tao C, Huang Z, Huang S (2010) Modeling of p53 signaling pathway based on S-system equations. Journal of Biomedical Engineering 27(3):505-10 (Chinese)
- [6]. Tavassoly I, Parmar J, Shajahan-Haq A, Clarke R, Baumann W, Tyson JJ (2015) Dynamic modeling of the interaction between autophagy and apoptosis in mammalian cells. CPT Pharmacometrics Syst Pharmacol 4(4):263-72.
- [7]. Battogtokh D, Kojima S, Tyson JJ (2018) Modeling the interactions of sense and antisense period transcripts in the mammalian circadianclock network. PLoS Comput Biol. <https://doi.org/10.1371/journal.pcbi.1005957>
- [8]. Tyson JJ, Novak B (2015) Models in biology: lessons from modeling regulation of the eukaryotic cell cycle. BMC Biol 13:46
- [9]. Heldt FS, Lunstone R, Tyson JJ, Nova'k B (2018) Dilution and titration of cell-cycle regulators may control cell size in budding yeast. PLoS Comput Biol. <https://doi.org/10.1371/journal.pcbi.1006548>
- [10]. Wu SJ, Chen WY, Chou CH, Wu CT (2013) Prototype of integrated pseudo-dynamic crosstalk network for cancer molecular mechanism. Math Biosci 243(1):81-98
- [11]. Chen X, Li X, Zhao W, Li T, Ouyang Q (2018) Parameter sensitivity analysis for a stochastic model of mitochondrial apoptosis pathway. PLOS ONE 13(6): e0198579. <https://doi.org/10.1371/journal.pone.0198579>
- [12]. Zi Z (2011) Sensitivity analysis approaches applied to systems biology models. IET Syst Biol. 5(6):336-6. doi: 10.1049/iet-syb.2011.0015. PMID: 22129029
- [13]. Borgonovo E and Plischke E. (2016) Sensitivity analysis: A review of recent advances. Eur. J. Oper. Res. 248(3):869-87. <https://doi.org/10.1016/j.ejor.2015.06.032>

- [14]. Sumner T, Shephard E and Bogle IDL. (2012) A methodology for global-sensitivity analysis of time-dependent outputs in systems biology modelling. *J. R. Soc. Interface* 2011(4):92156–2166. <http://doi.org/10.1098/rsif.2011.0891>
- [15]. Wang T, Wei Y and Jie. (2022) Global sensitivity analysis on debris flow energy dissipation of the artificial step-pool system, *Comput Geotech* 147:104758. <https://doi.org/10.1016/j.compgeo.2022.104758>
- [16]. Hu D, Yuan JM. (2006) Time-dependent sensitivity analysis of biological networks: coupled MAPK and PI3K signal transduction pathways. *J Phys Chem A*. 110(16):5361-70. doi: 10.1021/jp0561975. PMID: 16623463
- [17]. Wu WH, Wang FS and Chang MS (2008) Dynamic sensitivity analysis of biological systems. *BMC Bioinformatics* 9:S17. <https://doi.org/10.1186/1471-2105-9-S12-S17>
- [18]. Shiraishi F, Tomita T, Iwata M, Berrada A, Hirayama H (2009) A reliable Taylor-based computational method for the calculation of dynamic sensitivities in large-scale metabolic reaction systems: algorithm and software evaluation. *Math. Biosci.* 222(2):73-85. DOI: 10.1016/j.mbs.2009.09.001 PMID: 19747493
- [19]. Shiraishi F, Egashira M, Iwata M (2011) Highly accurate computation of dynamic sensitivities in metabolic reaction systems by a Taylor series method. *Math. Biosci.* 233(1):59-67. <https://doi.org/10.1016/j.mbs.2011.06.004>.
- [20]. Perumal TM, Gunawan R (2014) pathPSA: A dynamical pathway-based parametric sensitivity analysis. *Ind. Eng. Chem. Res.* 53(22):9149-9157. DOI: 10.1021/ie403277d
- [21]. Sriyudthsak K, Shiraishi F (2010) Selection of best indicators for ranking and determination of bottleneck enzymes in metabolic reaction systems. *Ind. Eng. Chem. Res.* 49(20):9738–9742. <https://doi.org/10.1021/ie100911h>
- [22]. Sriyudthsak K, Shiraishi F (2010) Identification of bottleneck enzymes with negative dynamic sensitivities: ethanol fermentation systems as case studies. *J Biotechnol.* 149(3):191-200. doi: 10.1016/j.jbiotec.2010.01.015
- [23]. Sriyudthsak K, Uno H, Gunawan R, Shiraishi F (2015) Using dynamic sensitivities to characterize metabolic reaction systems. *Math. Biosci.* 269:153-163. <https://doi.org/10.1016/j.mbs.2015.09.002>
- [24]. Callier, FM., Desoer CA. (1991). *Linear system theory*. New York : Springer-Verlag.
- [25]. <http://jij.biochem.sun.ac.za/database/silva/index.html>
- [26]. https://www.tutorialspoint.com/matlab_simulink/matlab_simulink_tutorial.pdf
- [27]. Sorribas A, Savageau MA. Strategies for representing metabolic pathways within biochemical systems theory: reversible pathways. *Math Biosci.* 1989;94(2):239-69. doi: 10.1016/0025-5564(89)90066-7. PMID: 2520170
- [28]. Liu PK, Wang FS (2008) Inverse problems of biological systems using multi-objective optimization. *J Chin Inst Chem Eng* 39(5):399-406. <https://doi.org/10.1016/j.jcice.2008.05.001>
- [29]. Wu SJ. (2021) Root locus-based stability analysis for biological systems. *J Bioinform Comput Biol* 19(5): 2150023. <https://doi.org/10.1142/S0219720021500232>

Supplement materials

A. Dynamic sensitivity for reversible pathways

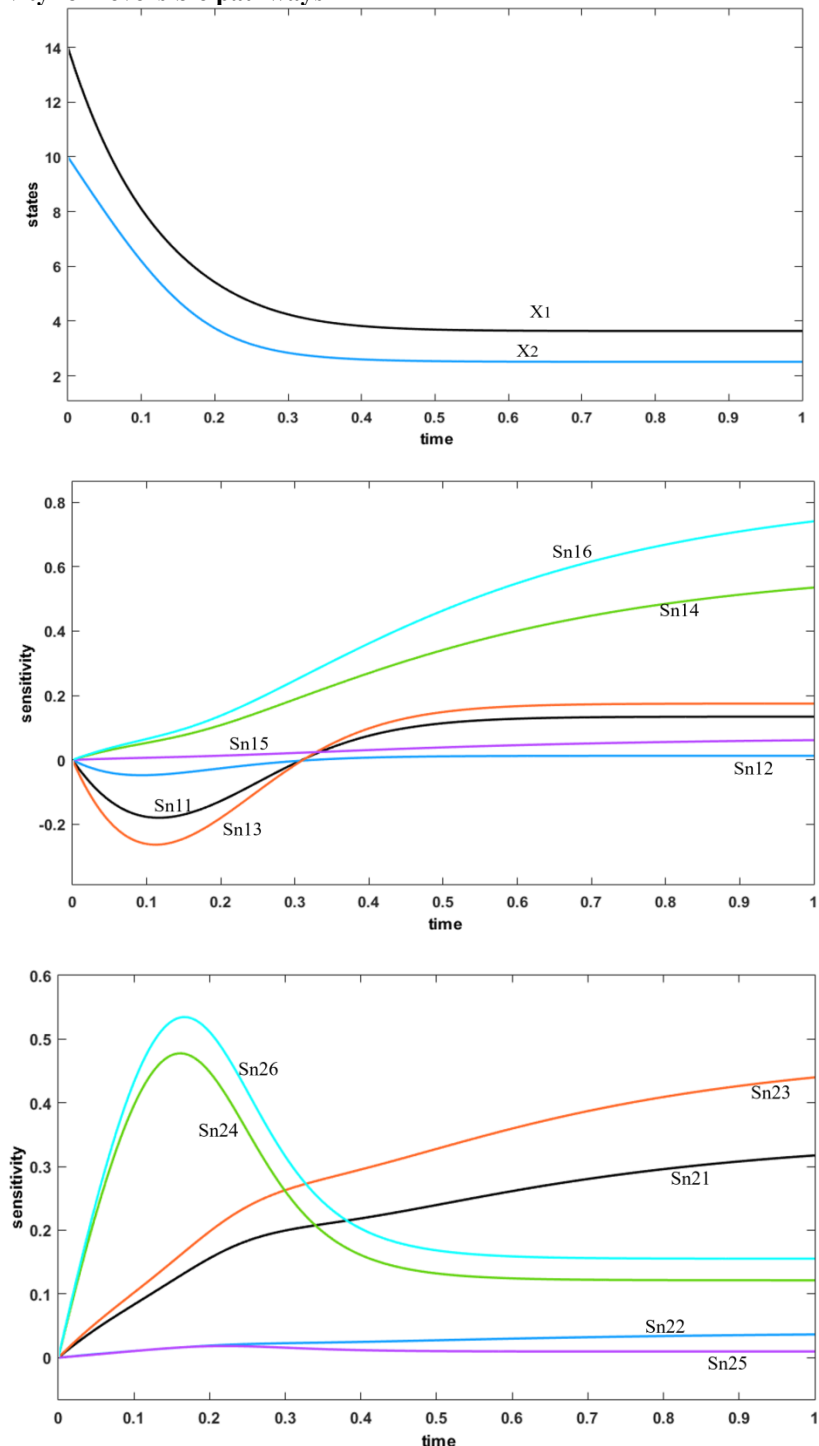


Figure S1: $((x_{10}, x_{20}, x_3, x_4) = (14, 10, 2, 4.8))$ Simulation results of system dynamic behavior (upper figure), sensitivity of x_1 (middle figure) and sensitivity of x_2 (down figure). $S_{n1i}, i = 1, \dots, 6$ denote the normalized sensitivity of x_1 to the parameters $K_{41}, K_{-41}, V_{41}^{max}, K_{12}, K_{-12}, V_{12}^{max}$ and $S_{n2i}, i = 1, \dots, 6$ denote the sensitivity of x_2 to the parameters $K_{12}, K_{-12}, V_{12}^{max}, K_{23}, K_{-23}, V_{23}^{max}$.

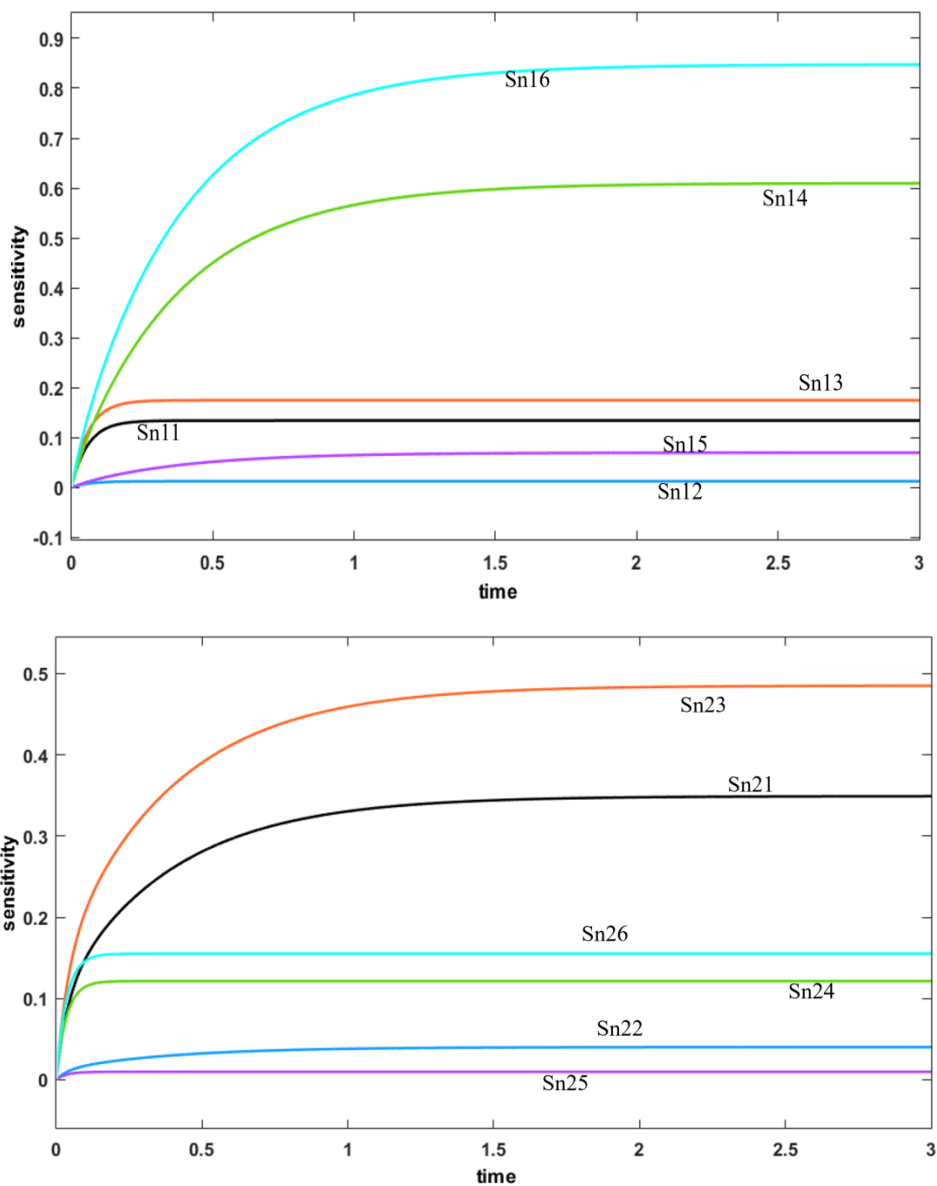
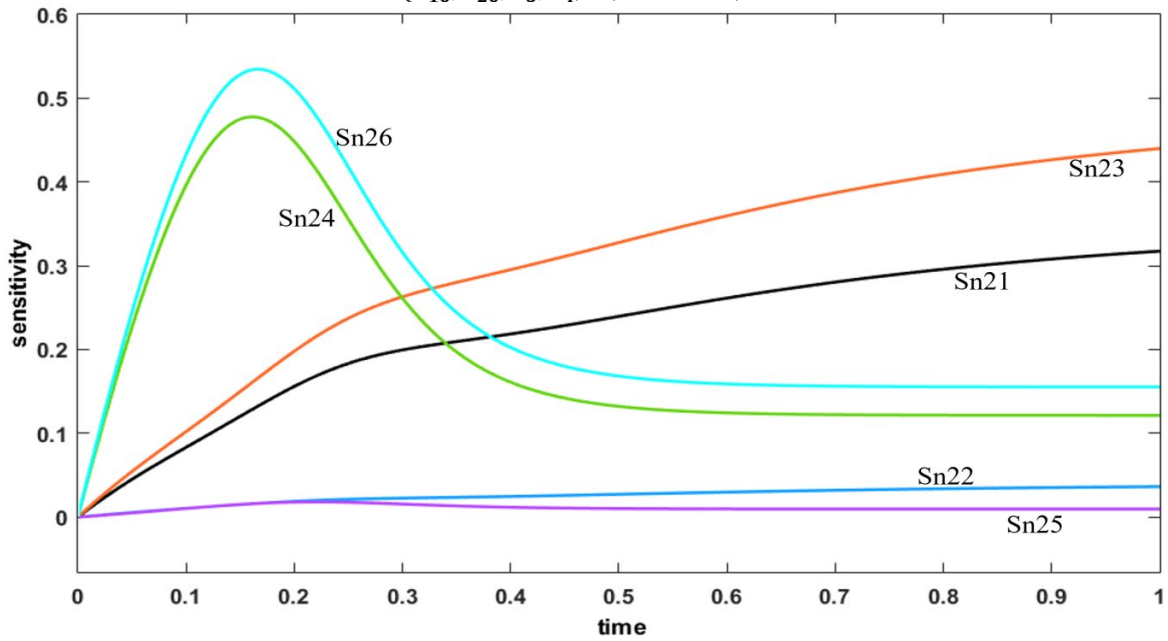


Figure S2: $((x_3, x_4) = (2, 4.8))$ Perturbation at steady states $(\bar{x}_1, \bar{x}_2) = (3.6384, 2.5113)$. Simulation results of sensitivity of x_1 (upper figure) and sensitivity of x_2 (down figure). $S_{n1i}, i = 1, \dots, 6$ denote the normalized sensitivity of x_1 to the parameters $K_{41}, K_{-41}, V_{41}^{max}, K_{12}, K_{-12}, V_{12}^{max}$ and $S_{n2i}, i = 1, \dots, 6$ denote the sensitivity of x_2 to the parameters $K_{12}, K_{-12}, V_{12}^{max}, K_{23}, K_{-23}, V_{23}^{max}$.

B. Comparison of Dynamic Sensitivity Evolution of S_{n2j}

$(x_{10}, x_{20}, x_3, x_4) = (14, 10, 2, 4.8)$



$(x_{10}, x_{20}, x_3, x_4) = (4, 3, 2, 4.8)$

